CENTRO DE INVESTIGACIONES EN ÓPTICA, A.C.

THEORETICAL STUDY OF THE GENERATION OF THREE ENTANGLED AND STEERABLE OPTICAL MODES BY A THIRD-ORDER NONLINEAR INTERACTION

MAESTRIA EN CIENCIAS (ÓPTICA)

Asesora: Laura Elena Casandra Rosales Zárate

Estudiante: Tarek Abraham Peña Armendáriz

Agosto de 2019
León, Guanajuato, México

De luz un haz, de fotones un mar.
Un vuelo ciego sin noción de tiempo y lugar,
y entre tanta relatividad
¿Cual será su realidad?
La trayectoria individual es caótica y coherente
¿Qué de ti será pequeño fotón?
Tu inmersión final es inminente
ahora vas al mar del famoso electrón.
Sigues un camino errante y esquivo,
y le apuestas al Quantum seguir vivo.
No hay manera de fallar
si la naturaleza hay que acatar.
Aun con el estruendo de creación y aniquilación,
no hay más que la conservación.
Tu energía, tiempo, momento y posición
tu descendencia llevará en correlación.

Esta tesis no hubiera sido realizada sin el apoyo de un gran numero de personas que me rodearon los últimos dos años y del CONACYT por su invaluable apoyo al permitirme ser uno de sus becarios para realizar mi maestría.

Miro mi reflejo en el espejo, mis expresiones, mi manera de hablar y no puedo dejar de ver a mi familia en mí. Inexorable soy a ellos, como igual mi agradecimiento eterno durante cada etapa de mi vida. Agradezco a mi padre Abraham por su fortaleza, a mi madre Esthela por su dedicación y a mis hermanas Katia y Diana por, a su manera, mostrarme que sin importa la adversidad, siempre hay nuevo amanecer.

Es muy común que el alumno agradezca a su asesor por el apoyo y guía que se le otorgó. Sin embargo, no fue hasta que trabaje con la Dra. Laura Elena Casandra Rosales Zárate que entendí el verdadero significado de esto. Gracias por el tiempo, por escuchar mis ideas, por los consejos, por enseñarme, por hacerme descubrir y entender, en fin gracias por haber sido la mejor asesora que pude haber pedido.

Dicen que la vida no se puede disfrutar si no se comparte, por lo tanto quiero agradecer al así llamado Club de los 5 que forme junto con Camilo, Mariana, Samuel y Juan. Todos y cada uno de ustedes hicieron que estos últimos dos años fueran una grata experiencia.

Laura, no puedo terminar esto sin agradecerte por tu grata compañía y porque, en más de una manera, me ayudaste a entender tantas cosas que, hasta anteriormente, permanecían desapercibidas por mí.

Finalmente, agradezco a mis amistades fuera del CIO que hicieron de este viaje una nueva aventura. Javier, Hiram, Sergio, Cesar, muchas gracias.

Contents

Abstract

The emergent quantum technologies have awoken a great scientific interest and effort to manipulate quantum systems. For these systems, quantum correlations are one of the characteristics on which emergent quantum technologies are based. It has been observed that in order to generate quantum correlations, as entanglement or EPR steering, non-linear optical devices are very useful. Even more, lately, generation of multipartite entanglement has become an important field of study for new applications on quantum protocols. One of the proposals to generate a genuine tripartite entangled state is to use a third-order nonlinear optical interaction. In this thesis we investigate three Hamiltonians for non-linear processes as third harmonic generation, spontaneous parametric down conversion, sum and difference of frequencies generation of third order. The Hamiltonians under consideration are composed of one high-frequency mode ($\hat{b}$) and low-frequency modes ($\hat{a}_i$). The difference between these three Hamiltonians is the freedom for the low-frequency modes to be strictly equals (one annihilation operator $\hat{a}^3$) or might be different ($\hat{a}_1^2\hat{a}_2$ or $\hat{a}_1\hat{a}_2\hat{a}_3$). In order to study these Hamiltonians and their capability to produce multipartite entanglement, we will use phase-space techniques and the theory of stochastic processes. Throughout this thesis, we will explain the mathematical framework of both theories and how they are connected. To certify entanglement and steering we use what are known as witnesses. Thus, we identify in which cases bipartite and multipartite entanglement are present. Finally, we found that bipartite entanglement and steering are always achieved for all the Hamiltonians under study. However, only in the case of $\hat{a}_1\hat{a}_2\hat{a}_3$ we found is possible to generate a tripartite steerable state in the three low-frequency modes and even more a four-modes entangled multicolored state.

1 Introduction

"Wir müssen wissen, Wir werden wissen."

"We must know, we will know."

David Hilbert 1862-1934

In the history of humanity there have been important developments and emergent technologies which, were landmarks due to the change they produced in human life. Must of the time this progress is a consequence of a deeper understanding of nature and/or the generation of new ideas that leads to a change in the scientific paradigm. One example of this are the quantum technologies. Despite of the idea that quantum technologies are just really new ideas which are still in development, we have been in contact with them for decades. At least for the so called first generation of quantum technologies.

The first generation of quantum technologies are the transistor-semiconductors devices and laser systems [1, 2]. There is no doubt about the importance of these inventions and in their contribution to the nowadays society. However, these kind of technologies are based on the effects of quantum mechanics but does not focus in the creation or manipulation of quantum states. In order to illustrate the actual meaning of this, lets consider a diode. The idea behind the diode is to allow the conduction in one direction and block it (very low conduction) in the other one. In order to do this, a voltage is applied. This voltage decreases or increases the depth of a quantum well in which the charges (electrons) are immersed. This is important for electronic systems, however, there is no interest in the state of the charges of the diode.

The second generation of quantum technologies (most of the times just called quantum technologies) are those ones where the main core are based on the quantum states and its properties [3, 4]. Therefore, explodes quantum effects as quantum superposition, entanglement and its correlations.

These new ideas are studied on the emergent fields of quantum information [5], quantum metrology [6, 7] and quantum communications [8]. Physical implementations of those are mostly based on quantum optics, atomic physics, quantum electronics or optoelectronics. In order to be able to manipulate such technologies, there must be a great capability to create and control quantum states with very specific properties.

Therefore, many research work have been made in the field. A commercial implementation of these technologies, as for example in quantum computing, has been pursuit highly in the last decade. The effort has been so great that the European scientific community released a manifesto in 2016, at the quantum Europe conference "to call to launch an ambitious European initiative in quantum technologies, needed to ensure Europe's leading role in a technological revolution now under way". In that manifesto they asked for one billion euros to their initiative [9]. Nevertheless, not only Europe is interested, worldwide companies as Google, Intel and IBM for example, have invested time, effort and significant quantities of money to create a universal quantum computer.

The reason behind all this interest in quantum computing is due to what its supremacy over classical computers. As an example, lets consider the nowadays security systems based of factorization. As it is known, any natural number can be factorized as a product of prime numbers. For example, $49 = 7^2$, $100 = 2^2 5^2$. However, the greater the number, the harder to find the correct factorization. These security systems use the factorization as the key to access to the protected information. Thus, the security relies on the incapability of a classical computer to solve the problem in an appropriate time. Nevertheless, despite the complexity, Shor showed a quantum algorithm which would be able to solve the problem in a quantum computer [10].

Thus, since quantum entanglement is a resource for these emergent technologies, its generation and correlation properties, are an important research area for both industrial and scientific development [11, 12, 13]. As we will explain later, it has been observed that a really efficient type of platforms used to generate entangled states are the optical ones. Before we go further on the subject we must give a briefly introduction to quantum entanglement.

This was introduced by Einstein, Podolsky and Rosen (EPR) in 1935 [14] in an attempt to show that quantum theory was incomplete and could not describe reality accurately. In their paper, EPR showed a continuous variable state, which is part of two subsystems A and B. For this state, after an interaction between each other, the final state could not be described as a product of independent states of the original subsystems. Even more, they showed, that this kind of states have the property that a measurement in A, can steer B. Such that B is be projected in a basis according to the measurement performed in A. The idea of being able to observe such an effect was enough evidence for EPR to conclude that quantum theory was incomplete. However, in response to that paper, Schrödinger introduced the terms of "entangled states" and "steering". Moreover, he said that entanglement was the characteristic of quantum mechanics and therefore quantum theory was not incomplete and, indeed, was complete and correct for local systems [15]. Nevertheless, he rejected the idea of non-local interactions.

In order to illustrate what a non-local interaction actually means, we show below the following example:

Let us consider the Hilbert space $\mathbb{C}^2 \otimes \mathbb{C}^2$ of two parties A and B with spin $|\uparrow\rangle$ or

$|\downarrow\rangle$ in the direction z. The state described as:

$$|\Psi\rangle = \frac{1}{\sqrt{2}}\Big(|\uparrow\downarrow\rangle + |\downarrow\uparrow\rangle\Big), \tag{1.1}$$

is one of the states known as Bell states, which are maximally entangled states. A measurement of the spin of party A will produce a collapse in the wave function. Such that, no matter the distance between parties A and B, party B must collapse to a definite state. Let us consider, as a matter of example, if the measurement of spin of A is $|\uparrow\rangle$ then, immediately the spin of B must collapse in $|\downarrow\rangle$. This failure of locality, was thought that it could not be observed. However in 1964, John Bell [16] introduced a set of inequalities, such that if quantum entanglement was a misleading subject of quantum theory, they must never be violated. These inequalities were named after him, it is worth to say that nowadays they have been violated several times[17, 18, 19, 20, 21, 22, 23, 24, 25, 26, 27].

The very first experiment about the violation of Bell-type inequalities [17], was performed by Freedman and Clauser in 1972 measuring the polarization of photons [18]. However, they used a variation of the Bell inequalities named Freedman's inequality. After that, Aspect *et al* [19] conducted the first three Bell's test, using calcium cascade sources [19, 20], where they showed violation of the Bell's inequalities. Later on, different Bell test were developed using different systems [21, 22]. However, there was the possibility of "loopholes" in these experiments. In 2015, three different groups were able to show significant loophole-free Bell-tests. The first one, performed by Hensen *et al* [23], demonstrated quantum entanglement in the spin of electrons at a distance of 1.3 km. That same year, Shalm *et al* [24] and Giustina *et al* [25] performed experiments with entangled photons. Remarkable was that Shalm's experiment used random number generators to choose the direction of the measurement basis. In 2018 two new experiments were carried out, with two new different approaches. The first one, by a great international collaboration, where instead of using random number generator, they used random human choices to choose the basis of measure. In order to did that, around 100,000 persons were recruited [26]. The second one, used light from two distant quasars to set the basis of their measurement settings [27]. These experiments showed that quantum entanglement is a correct feature of quantum mechanics.

With the purpose of illustrate the meaning of steering lets consider again the state of Eq. (1.1). This state may be written in the basis generated by the Pauli's matrix $\hat{S}_z$ as in the first example, or it can be expressed in the direction of x, i.e., the basis generated by $\hat{S}_x$. If the eigenstates in the direction of x are $|+\rangle$ or $|-\rangle$, then the state may be written as:

$$|\Psi\rangle = \frac{1}{\sqrt{2}}\Big(|+-\rangle + |-+\rangle\Big), \tag{1.2}$$

So far, this is no more but two different ways to represent a state. However, at the moment of performing a measurement on one of the parties, the remaining part is projected in the chosen basis by the other party. Thus, lets consider a measurement on party A. We will, obtain the to following different outcomes for party B:

$$\text{if} \begin{cases} \hat{S}_z, & \hat{\rho} = \frac{1}{2}\left(|\uparrow\rangle\langle\uparrow| + |\downarrow\rangle\langle\downarrow|\right), \\ \hat{S}_x, & \hat{\rho} = \frac{1}{2}\left(|+\rangle\langle+| + |-\rangle\langle-|\right). \end{cases}$$

These different results imply that it is possible to *steer* the final state of party B, reason why Schrödinger has referred to it as "steering". It has been observed that such a resource is important for quantum teleportation [28] and quantum cryptography [29, 30].

Steering and quantum entanglements are two important quantum resources which potential applications to quantum information. Thus, much work has been done in order to quantify and certify them [12, 11, 31, 32, 33, 34]. On the other hand, besides the scientific investigations on the verification of quantum entanglement and its implementation, there have also been studies on the generation of multipartite entanglement. This has been already achieved in different platforms, for instance for a Greenberger–Horne–Zeilinger (GHZ) state of 14 ions [35], generation of tripartite entanglement by optical means [36, 37, 38, 39, 40, 41, 42, 43, 44] and recently in quantum memories [45]. Nowadays, as far as we are concerned, there is no standard method to experimentally generate entangled states of four and three modes, therefore, this remains as an open research area. Moreover, there have also been theoretical investigations for tripartite entanglement generation [46, 47, 48]. In particular, the proposal of Rojas *et al* [47] used a third-order nonlinear interaction to produce tripartite entanglement.

Thus, our goal is to study an optical system to generate genuine multipartite entangled and steerable states. In order to do so, we will study the third-order non-linear interaction proposed by Rojas *et al* [47] but in its most general form. Even though in their study they found generation of tripartite entanglement, their approach is performed under the undepleted approximation, i.e., the pump beam (high-frequency mode, HF) is treated as a classical beam. This approximation makes not possible to investigate the quantum correlations that HF mode might have. In addition, quantum steering is not investigated.

Thus, we investigate this third-order nonlinear interaction, but, the undepleted approximation is not considered. This new approach allow us to treat the high-frequency mode as a quantum one. Thus, besides tripartite entanglement between the low-frequency (LF) modes, we can study entanglement with the HF mode. In particular, we show that this non-linear interaction might produce a four modes entangled state. Moreover, we also show certification of bipartite and tripartite steering.

Throughout this thesis, we must give a briefly introduction to quantum entanglement and steering witnessing. After that, we will describe the mathematical framework of quantum optics which was used in this work. Then, we will explain the optical system which we proposed to generate entanglement and our results.

2 Quantum correlations

"If a man never contradicts himself, the reason must be that he virtually never says anything at all."

Erwin Schrödinger 1887-1961

Referring to quantum correlations we must distinguish between the different types and characteristics. In this thesis, we considered entanglement and steering.

2.1 Quantum Entanglement

Lets define a system in a Hilbert space $\mathcal{H}$, which can be described as a direct product of two subspaces $\mathcal{H}_1$ and $\mathcal{H}_2$, $\mathcal{H} = \mathcal{H}_1 \otimes \mathcal{H}_2$. In the case of pure states where $|\Psi\rangle$ is a state in $\mathcal{H}$ such that it can not be written down as:

$$|\Psi\rangle = |\psi_1\rangle|\psi_2\rangle, \tag{2.1}$$

where $|\psi_1\rangle$ and $|\psi_2\rangle$ are states in $\mathcal{H}_1$ and $\mathcal{H}_2$ respectively, then the state is entangled.

In the case of general states, which include the mixed states, we consider a density operator $\hat{\rho}$ in $\mathcal{H}$. If there are density operators $\hat{\rho}_i^1$, and $\hat{\rho}_i^2$ in $\mathcal{H}_1$ and $\mathcal{H}_2$ respectively, such that it is possible to write:

$$\hat{\rho} = \sum_i \omega_i \hat{\rho}_i^1 \hat{\rho}_i^2, \tag{2.2}$$

where ω_i are probabilities, then the state is separable, if this is not true the state is entangled.

2.2 Steering

Now we show the way in which EPR argued about the completeness of quantum mechanics. As above, we define a system $\mathcal{H}$ which can be described as the direct product of two subsystems $\mathcal{H}_1$ and $\mathcal{H}_2$. Now lets consider an state $|\Psi\rangle$ in $\mathcal{H}$ such that:

$$|\Psi\rangle = \sum_{n=0}^{\infty} |\psi_1\rangle_n |\psi_2\rangle_n = \sum_{m=0}^{\infty} |\phi_1\rangle_m |\phi_2\rangle_m, \tag{2.3}$$

where $|\psi_1\rangle_n$ and $|\phi_1\rangle_m$ are states in $\mathcal{H}_1$ and $|\psi_2\rangle_n$, $|\phi_2\rangle_m$ in $\mathcal{H}_2$. Now, lets consider two operators $\hat{S}$ and $\hat{T}$ which do not commute. If $|\psi_i\rangle_n$ are eigenstates of $\hat{S}$ and $|\phi_i\rangle_m$ eigenstates of $\hat{T}$. It is possible to perform a measurement in one subsystem, lets say $\mathcal{H}_1$, according with the measure the state will collapse either in the basis of $\hat{S}$ or $\hat{T}$, i.e., in $|\psi_1\rangle_n$ or $|\phi_1\rangle_m$. However, this will not be on both, such that the other subsystem $\mathcal{H}_2$ must collapse also in $|\psi_2\rangle_n$ or $|\phi_2\rangle_m$. In that way, measuring one subsystem must steer the other one.

It is important to clarify that the set of steerable states is a strict subset of the set of entangled states [49, 50].

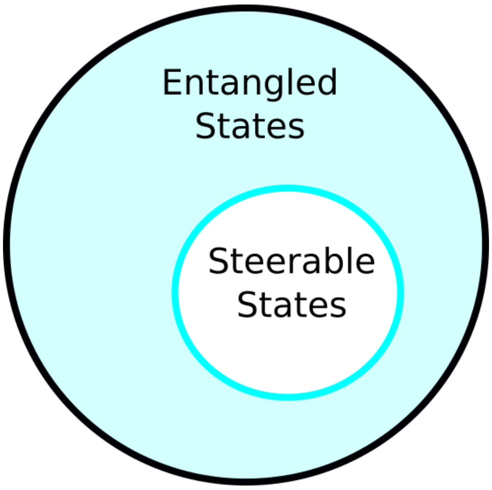

Figure 2.1: Venn diagram of entangled and steerable states.

2.3 How to certify entanglement and steering

The study of quantum entanglement require the capability of distinguish which states are entangled and which are not. Therefore, a great effort has been made to develop criteria to measure the amount of entanglement and to identify it. In this thesis we focus in how to identify it, rather than to measure the amount of it. These criteria are called witnesses. This is because these criteria witness entanglement, but do not quantify how much entanglement is between the parties. In addition, it may happen that a witness do not identify an entangled state. For that reason, we shall never say that a state is not entangled if a witness do not identify it as such. On the other hand, entanglement it is not restricted to bipartite systems, as matter of fact, it might take place in any multipartite system. Thus, we shall describe different criteria that are used to study bipartite and n-parties systems. In this work we focus in continuous variables systems. This means that the degrees of freedom in which the state might be entangled, take continuous values.

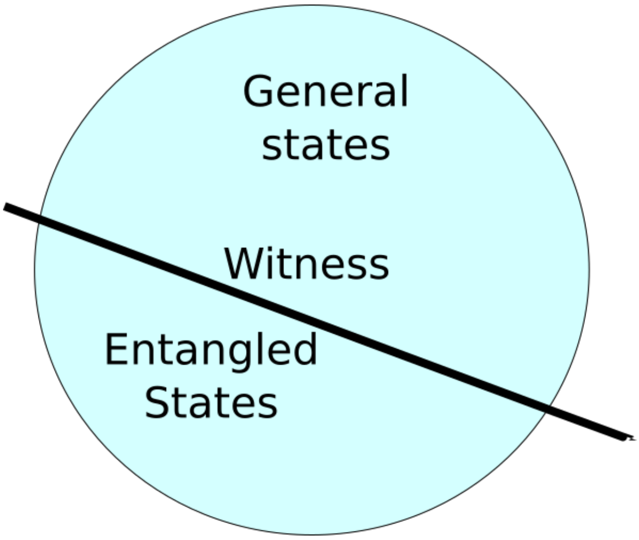

Figure 2.2: Representation of a witness certifying entanglement.

2.3.1 Bipartite systems

For the case of continuous variable systems, where there are only two distinguishable subsystems, two main criteria are considered. We discuss both of them below.

Duan, Giedke, Cirac and Zoller-Simon criterion

One of the inequalities that is used to certify that a state is entangled, was developed by Duan, Giedke, Cirac and Zoller (DGCZ) [51] and Simon [52]. Using the field quadratures operators $\hat{X} = (\hat{a}+\hat{a}^\dagger)/2$ and $\hat{P} = (\hat{a}-\hat{a}^\dagger)/2i$ with $\left[\hat{X}_l, \hat{P}_k\right] = \frac{i}{2}$, where $\hat{a}(\hat{a}^\dagger)$ is the annihilation (creation) operator. Then the inequalities are given by:

$$\begin{aligned} \Delta^- = \Delta^2(\hat{X}_i - \hat{X}_j) + \Delta^2(\hat{P}_i + \hat{P}_j) &\geq 4, \\ \Delta^+ = \Delta^2(\hat{X}_i + \hat{X}_j) + \Delta^2(\hat{P}_i - \hat{P}_j) &\geq 4. \end{aligned} \tag{2.4}$$

Here $\Delta^2(\hat{A})$ is the variance of the operator $\hat{A}$. The violation of any of these inequalities certify the existence of bipartite entanglement.

V. Giovannetti, S. Mancini, D. Vitali, and P. Tombesi criterion

Giovanetti *et al* [53] developed the second criterion that we will use. The criterion states that if:

$$Ent(g_x, g_p) = \frac{\sqrt{\Delta^2(\hat{X}_i - g_x\hat{X}_j)\Delta^2(\hat{P}_i + g_p\hat{P}_j)}}{(1 + g_x g_p)} \geq 1, \tag{2.5}$$

does not hold, then the bipartite state is entangled.

Here g_x and g_p are real parameters which are chosen optimally. If g_x=g_p, is called the symmetric case ($g^{(sym)}$) and we denote $Ent(g_x, g_p) \equiv Ent(g^{(sym)})$. Here we will take two different $g^{(sym)}$ such that $Ent(1) = Ent^-$ and $Ent(-1) = Ent^+$.

Bipartite Steering

In order to certify steering the criteria developed by Reid [54] will be used, which is:

$$E_{i|j} = V_{inf|j}(\hat{X}_i)V_{inf|j}(\hat{P}_i) < 1, \tag{2.6}$$

where:

$$\begin{aligned} V_{inf|j}(\hat{X}_i) &= \Delta^2(\hat{X}_i) - \frac{[\Delta^2(\hat{X}_i, \hat{X}_j)]^2}{\Delta^2(\hat{X}_j)}, \\ V_{inf|j}(\hat{P}_i) &= \Delta^2(\hat{P}_i) - \frac{[\Delta^2(\hat{P}_i, \hat{P}_j)]^2}{\Delta^2(\hat{P}_j)}. \end{aligned}$$

Here $\Delta^2(\hat{A}, \hat{B}) = \left\langle \left(\hat{A}\hat{B} + \hat{B}\hat{A}\right)/2 \right\rangle - \left\langle \hat{A} \right\rangle \left\langle \hat{B} \right\rangle$, is the covariance of operators $\hat{A}$ and $\hat{B}$.

One conclusion that we might obtain for the three last witnesses is that while entanglement is symmetric, steering is not. Thus, in a composite system made by two recognizable modes, lets say A and B. It is possible that mode A steers mode B, but B does not steer A.

2.3.2 Multipartite systems

Before we explain the theory of multipartite witnesses, some clarifications will be explained. When we are interested in a system of N parties, where $N \geq 3$, we must make a distinction between genuine N-partite entanglement and fully inseparable states [55]. For the sake of clarity, we study the following state of three parties:

$$\hat{\rho} = P_1 \sum_i \omega_i \hat{\rho}_{12}\hat{\rho}_3 + P_2 \sum_n \omega_n \hat{\rho}_1\hat{\rho}_{23} + P_3 \sum_m \omega_m \hat{\rho}_{13}\hat{\rho}_2, \tag{2.7}$$

where $\sum P_i = 1$ and $\sum \omega_k = 1$. $\hat{\rho}_{ij}$ are density operators of the composite system $\mathcal{H} = \mathcal{H}_i \otimes \mathcal{H}_j$ and $\hat{\rho}_k$ a density operator in $\mathcal{H}_k$. This state is not genuinely entangled in its three parties. Even when $\hat{\rho}_{ij}$ may be density operators of bipartite entangled states. Therefore, a genuine three-party entangled state is that one which cannot be written as Eq. (2.7). However, if $\hat{\rho}_{ij}$ are entangled states, $\hat{\rho}$ would be fully inseparable.

Once we have said the above, we show the criteria that are used for this situation.

P. van Loock and A. Furusawa

Peter van Loock and Akira Furusawa [56] have derived sufficient conditions to detect multiparty entangled states. Since in this thesis, we focus on tripartite quantum correlations, we will only show the theory for the tripartite state case.

First, let us define the following operators:

$$\hat{U} = h_1\hat{x_1} + h_2\hat{x_2} + h_3\hat{x_3}, \tag{2.8}$$
$$\hat{V} = g_1\hat{p_1} + g_2\hat{p_2} + g_3\hat{p_3}. \tag{2.9}$$

Here h_i and g_i are real parameters chosen optimally. Now let us suppose a state given by,

$$\hat{\rho} = \sum_i \eta_i \hat{\rho}_{i,km} \otimes \hat{\rho}_{i,n}, \tag{2.10}$$

here $\hat{\rho}_{i,km}$ means that party k may be entangled with m, but none of them is entangled with n. The sum of the variances of $\hat{u}$ and $\hat{v}$ is:

$$\begin{aligned}\langle(\triangle\hat{U})^2\rangle_\rho + \langle(\triangle\hat{V})^2\rangle_\rho = \sum_i \eta_i \Big[& h_k^2\langle x_k^2\rangle + h_m^2\langle x_m^2\rangle + h_n^2\langle x_n^2\rangle \\ & + 2\Big[h_k h_n\langle x_k x_n\rangle + h_k h_m\langle x_k x_m\rangle + h_n h_m\langle x_n x_m\rangle\Big] \\ & + g_k^2\langle p_k^2\rangle + g_m^2\langle p_m^2\rangle + g_n^2\langle p_n^2\rangle \\ & + 2\Big[g_k g_n\langle p_k p_n\rangle + g_k g_m\langle p_k p_m\rangle + g_n g_m\langle p_n p_m\rangle\Big]\Big] \\ & - \langle\hat{u}\rangle_\rho^2 - \langle\hat{v}\rangle_\rho^2.\end{aligned} \tag{2.11}$$

Now, since we have said that party n is not entangled with k and m, it is possible to write $\langle x_k x_n\rangle$ as a separation of products given by $\langle x_k\rangle\langle x_n\rangle$. Similarly, for the terms of n with m and k. However, we can not do the same between k and m. Using this separation in Eq. (2.11) we get:

$$\begin{aligned}\langle(\triangle\hat{u})^2\rangle_\rho + \langle(\triangle\hat{v})^2\rangle_\rho = \sum_i \eta_i\Big[&\langle x_k^2\rangle + h_m^2\langle x_m^2\rangle + h_n^2\langle x_n^2\rangle + g_k^2\langle p_k^2\rangle + g_m^2\langle p_m^2\rangle + g_n^2\langle p_n^2\rangle \\ &+ 2\Big[h_k h_m \Delta^2(x_k, x_m) + h_k h_n \cancel{\Delta^2(x_k, x_n)} + h_m h_n \cancel{\Delta^2(x_m, x_n)} \\ &+ g_k g_m \Delta^2(p_k, p_m) + g_k g_n \cancel{\Delta^2(p_k, p_n)} + g_m g_n \cancel{\Delta^2(p_m, p_n)}\Big]\Big] \\ &\sum_i \eta_i \langle\hat{u}\rangle_i^2 - (\sum_i \eta_i\langle\hat{u}\rangle_i)^2 \sum_i \eta_i\langle\hat{v}\rangle_i^2 - (\sum_i \eta_i\langle\hat{u}\rangle_i)^2.\end{aligned} \tag{2.12}$$

Now, for the next step we are going to use the following relations:

$$\langle\triangle\hat{A}^2\rangle + \langle\triangle\hat{B}^2\rangle \;\; \geq \;\; |\langle[\hat{A}, \hat{B}]\rangle|, \tag{2.13}$$

$$\Big[\hat{X}_l, \hat{P}_k\Big] = ic\delta_{kj}, \tag{2.14}$$

where c is a constant related to the normalization factor. Next, we notice that the last line in Eq. (2.12) is always not negative, due to the inequality of Cauchy-Schwarz, we can rewrite it as:

$$\begin{aligned}&\sum_i \eta_i\Big[h_k^2\langle x_k^2\rangle + h_m^2\langle x_m^2\rangle + h_n^2\langle x_n^2\rangle + g_k^2\langle p_k^2\rangle + g_m^2\langle p_m^2\rangle + g_n^2\langle p_n^2\rangle \\ &+ 2\Big[h_k h_m \Delta^2(x_k, x_m) + g_k g_m \Delta^2(p_k, p_m)\Big]\Big] \\ &= h_n^2\langle\triangle x_n^2\rangle + g_n^2\langle\triangle g_n^2\rangle + \langle\triangle(h_k x_k + h_m x_m)^2\rangle + g_n^2\langle\triangle(g_k p_k + g_m p_m)^2\rangle \\ &\geq \mid \langle\Big[h_n x_n, g_n p_n\Big]\rangle \mid + \mid \langle[h_k x_k + h_m x_m, g_k p_k + g_m p_m]\rangle \mid \\ &= c\Big[\mid h_n g_n \mid + \mid h_k g_k + h_m g_m \mid\Big].\end{aligned} \tag{2.15}$$

Throughout this thesis, $c = \frac{1}{2}$. Therefore, if Eq. (2.15) does not hold, the tripartite state is genuine entangled for pure states. While for mixed states, the state is said to be at least fully inseparable.

R.Y. Teh and M. D. Reid criterion

In order to certify genuine multipartite entanglement and steering for general states, the criterion developed in [55] must be used. Violation of the following inequality confirms genuine tripartite entanglement and steering:

$$\begin{aligned} S = \Delta^2(\hat{U}) + \Delta^2(\hat{V}) \quad &\geq \quad C\, min\{|h_3 g_3| + |h_1 g_1 + h_2 g_2|], \\ &\quad\quad |h_2 g_2| + |h_1 g_1 + h_3 g_3|, \\ &\quad\quad |h_1 g_1| + |h_2 g_2 + h_3 g_3|\}. \end{aligned} \tag{2.16}$$

This inequality corresponds to the case of entanglement when $C = 2$, while it corresponds to steering for $C = 1$.

In this thesis we take $h_1 = h_2 = h_3 = g_1 = 1$, $g_2 = g_3 = -1/2$, which set the inequality as:

$$\Delta^2\left[\hat{X}_1 + \hat{X}_2 + \hat{X}_3\right] + \Delta^2\left[\hat{P}_1 - \frac{(\hat{P}_2 + \hat{P}_3)}{2}\right] \geq C. \tag{2.17}$$

2.4 Monogamy relations

Lets consider a system which is composed of more than two distinguishable subsystems. Lets say A, B and C, in such a case it is possible to study bipartite entanglement and steering in pairs. In order to do this, we will use the so called monogamy relations. Here we use monogamy relations developed in [57]:

$$E_{B|A} E_{B|C} \geq max\{1, E^2_{B|\{AC\}}\}, \tag{2.18}$$

where $\{AC\}$ is the composite system of A and B. A consequence of this relation is that, if it is possible to certify steering from A to B, then $E_{B|C}$ would not be capable to certify steering from C to A.

In addition, there are two other monogamy relations for the entanglement witnesses derived in [58]:

$$Ent_{B|A} Ent_{B|C} \geq \frac{max\left\{1, E^2_{B|\{AC\}}\right\}}{\left[1 + (g^{(sym)}_{BA})^2\right]\left[1 + (g^{(sym)}_{BA})^2\right]}, \tag{2.19}$$

$$\Delta_{B|A} \Delta_{B|C} \geq max\left\{1, E_{B|\{AC\}}\right\}. \tag{2.20}$$

Here $\Delta_{B|A}$ denotes the Duan et al criterion defined in Eq. (2.4). These two last relations establish bounds for the entanglement witnessing.

3 Coherent states and Phase-space picture

"Somewhere, something incredible is waiting to be known."

Carl Sagan 1934-1996

3.1 Coherent states

The quantized electric field, in the Heisenberg representation, is expressed in terms of the creation and annihilation operators in the following form [59]:

$$\hat{E}(\vec{r},t) = i\sum_k \sqrt{\frac{\hbar\omega_k}{2V\epsilon_o}}\vec{e_k}\Big(\exp(i\vec{k}\cdot\vec{r})\hat{a}_k(t) - \exp(-i\vec{k}\cdot\vec{r})\hat{a}_k^\dagger(t)\Big), \tag{3.1}$$

where $\vec{k}$ is the number wave vector, $\vec{r}$ the position vector, $\vec{e_k}$ the unitary polarization vector, V the volume of quantization, and ϵ_o is the permissibility of vacuum.

Thus, the properties of the electric field may be calculated as expectation values of combinations and products of both operators.

It is easy to show that for a number or Fock state $\langle n|\hat{E}|n\rangle = 0$. Therefore, in order to find the classical limit of the field (mean field different to zero) we must seek states for which mean field do not vanish (as it happen with the number states). In other words, it is necessary to find the eigenstates of the annihilation operator.

Those states are called coherent states [60], they are represented as $|\alpha\rangle$ and obey the following relation:

$$\hat{a}|\alpha\rangle = \alpha|\alpha\rangle. \tag{3.2}$$

It is easy to find that these states also satisfy:

$$\langle\alpha|\hat{a}^\dagger = \alpha^*\langle\alpha|. \tag{3.3}$$

The coherent states have the property, as the vacuum state, that they minimize the Heisenberg uncertainty relation for the field quadratures, which is $\langle\triangle\hat{X}_1{}^2\rangle\langle\triangle\hat{X}_2{}^2\rangle \geq$

$\frac{1}{16}$. This means that a coherent state minimize the quantum noise, remaining only the noise due to the vacuum. This property is stated as:

$$\langle \triangle \hat{X}_1{}^2 \rangle_\alpha = \langle \triangle \hat{X}_2{}^2 \rangle_\alpha = \frac{1}{4}. \tag{3.4}$$

It makes perfect sense that coherent states minimize the uncertainty principle, since we were seeking states for the classical limit. Thus, the coherent states are the most classical like quantum states.

Even more, since the expectation value of the number operator is

$$\langle \hat{N} \rangle_\alpha = |\alpha|^2, \tag{3.5}$$

coherent states has a continuous expectation value of number of photons, as it would be expected in the classical picture.

There are two important properties for the coherent states. These are the completeness relation or resolution of unity and their inner product. These are given below:

$$\int |\alpha\,\rangle\langle\,\alpha| \frac{d^2\alpha}{\pi} = 1. \tag{3.6}$$

$$\langle \beta | \alpha \rangle = \exp\Big[\frac{1}{2}(\beta^* \alpha - \beta \alpha^*)\Big] \exp\Big[-\frac{1}{2}|\beta - \alpha|^2\Big]. \tag{3.7}$$

Coherent states form an over complete basis for the Hilbert space of one single-mode electromagnetic field. This means that any state can be represented as a combination of coherent sates. However this combination might not be unique.

3.2 Phase-Space Representation

Unlike classical mechanics, quantum mechanics do not accept the classic idea of phase-space, since the operators $\hat{X}$ and $\hat{P}$ do not commute. However, it is possible to use the properties of coherent states to construct a complex plane working as a phase-space. Using the field quadratures operators we find:

$$\langle \hat{X}_1 \rangle_\alpha = \frac{(\alpha + \alpha^*)}{2} = Re(\alpha), \qquad \langle \hat{X}_2 \rangle_\alpha = \frac{(\alpha - \alpha^*)}{2i} = Im(\alpha). \tag{3.8}$$

In that way it is possible to use the α-plane as a phase-space.

3.2.1 Phase-space probability quasidistributions

There are several functions which are part of the set of phase-space probability quasidistributions, which are also known as phase-space representations. However, in this thesis we focus only in three of them. Bellow we introduce th P-function, the positive-P and the Wigner functions.

3.2.1.1 P-function

Since coherent states form a continuous basis, it is possible to express the density operator $\hat{\rho}$, in terms of a function $P(\alpha)$, as:

$$\hat{\rho} = \int P(\alpha) \, |\alpha\rangle\langle\alpha| \, d^2\alpha, \tag{3.9}$$

This P-function is known as the Glauber-Sudarshan P-function [60]. This P-function might be considered as a probability distribution. However, since this distribution may be negative in certain regions, it should not be called a probability distribution but a quasi-distribution. Before we show the usefulness of this function, we shall show how it can be calculated. Given a density operator, the P-function is obtained by using:

$$P(\alpha) = \frac{e^{|\alpha|^2}}{\pi^2} \int e^{|u|^2} \langle -u \, |\hat{\rho}| \, u\rangle \, e^{u^*\alpha - u\alpha^*} d^2u. \tag{3.10}$$

Now, one of the greatest strength of P-function relies in the following theorem

Optical equivalence theorem of Sudarshan

Lets define a normally ordered function $\hat{G}^{(N)}(\hat{a}, \hat{a}^\dagger)$, i.e., all the powers of $\hat{a}^\dagger$ are in the left side respect $\hat{a}$. Hence we consider the following form:

$$G^{(N)}(\hat{a}, \hat{a}^\dagger) = \sum_n \sum_m c_{nm} \hat{a}^{\dagger n} \hat{a}^m. \tag{3.11}$$

Next, using the expansion of the density matrix in terms of the P-function given in Eq. (3.9), expectation values can be obtained as [61]:

$$\left\langle G^{(N)}(\hat{a}, \hat{a}^\dagger) \right\rangle = \int P(\alpha) G^{(N)}(\alpha, \alpha^*). \tag{3.12}$$

The optical equivalence theorem provides a useful way to compute expectation values of normally ordered operators weighting P-function with $G^{(N)}$.

3.2.2 Positive P function

At this point, the importance of such a function is more clear. However, as we have described above, the P-function is not positive semidefinite and even for some cases it is not well-behaved. The last may bring problems in certain treatments concerned to this thesis. Reason why, we now must proceed to introduce a more general representation which would be well-behaved and positive semidefinite. This distributions was introduced by P. D. Drummond C. Gardiner [62], is called positive P-function and is defined through the following relation:

$$\hat{\rho} = \int P^{+}(\alpha, \alpha^{+})\hat{\Lambda}(\alpha, \alpha^{+})d^2\alpha d^2\alpha^{+}, \tag{3.13}$$

where

$$\hat{\Lambda}(\alpha, \alpha^{+}) = \frac{|\alpha\,\rangle\langle\,\alpha^{+}|}{\langle\alpha^{+}|\alpha\rangle}. \tag{3.14}$$

The first situation to note is that positive-P function is integrated over a space of two independent complex variables, unlike the P function. This double the complex space. In addition, the fact that α and α^{+} are independent variables allow us to cover the whole complex plane. This provides the opportunity to choose a function P^{+} that is always positive semidefinite. Therefore it behaves like an actual probability distribution.

An important fact is that the optical equivalence theorem remains in the way of:

$$\left\langle G^{(N)}(\hat{a}, \hat{a}^{\dagger})\right\rangle = \int P(\alpha, \alpha^{+})G^{(N)}(\alpha, \alpha^{+}). \tag{3.15}$$

3.2.3 Wigner function

Finally we shall introduce the Wigner function which was the very first quasi-distribution probability (in a Quantum mechanics context). In 1932, in an attempt to introduce a probability distribution in the phase space, Wigner came up with a function, that later on was named after him.

The Wigner function is defined as:

$$W(q,p) \equiv \frac{1}{2\pi\hbar}\int_{-\infty}^{\infty}\left\langle q + \frac{1}{2}x\middle|\hat{\rho}\middle|q - \frac{1}{2}x\right\rangle e^{ipx/\hbar}dx.$$

For pure states, the Wigner function is closely related to the wave function. This function depends on two parameters, q and p. In the case where q and p are position and momentum parameters, we can obtain the probability density for each representation, by integrating as follows:

$$\int_{-\infty}^{\infty} W(q,p)dq = |\varphi(p)|^2, \tag{3.16}$$

and

$$\int_{-\infty}^{\infty} W(q,p)dp = |\psi(q)|^2. \tag{3.17}$$

If it is true $|\varphi(p)|^2$ and $|\psi(q)|^2$ are probability densities, Wigner function is not. $W(q,p)$ may be negative in certain regions. Nevertheless, as the last two distributions, it can be used to calculate expectation values, but, this time, for Weyl (symmetrically) ordered operators.

In order to illustrate the meaning of symmetric order we must show an example:

$$\begin{aligned} (\hat{a}^\dagger \hat{a})_s &= \frac{1}{2}(\hat{a}^\dagger \hat{a} + \hat{a}\hat{a}^\dagger), \\ (\hat{a}^{\dagger^2} \hat{a})_s &= \frac{1}{3}(\hat{a}^{\dagger^2} \hat{a} + \hat{a}^\dagger \hat{a}\hat{a}^\dagger + \hat{a}\hat{a}^{\dagger^2}), \end{aligned} \tag{3.18}$$

and so on.

So that, if we have a symmetrically ordered operator, lets say $\{G(\hat{q},\hat{p})\}_W$ then

$$\Big\langle \{G(\hat{q},\hat{p})\}_W \Big\rangle = \int \{G(q,p)\}_W \, W(q,p) dq dp. \tag{3.19}$$

3.3 Mapping von Neumann equation to Phase-space representations

Time evolution of quantum systems is given by the von Neumann equation given below:

$$\frac{\partial \hat{\rho}}{\partial t} = -i\hbar[\hat{H}_{int}, \hat{\rho}]. \tag{3.20}$$

The solution of this equation is enough to obtain all the properties of the system. Nevertheless, most of the time, this solution is not easy to find. Therefore, it is necessary to use other approaches to solve the problem. Here, we focus in the use of the phase-space representations to find a solution [63]. The use of this methods have been used in quantum optics in a wide range of platforms [64, 65, 66, 67, 68, 69, 70, 71, 72]. The idea is to write a time evolution equation for the quasi-distribution functions. There are mappings to obtain differential equations for the phase-space representations from the Eq. (3.20). In the case of the positive-P and Wigner representations, those mappings are showed below:

$$\begin{aligned} \hat{a}\hat{\rho} &= \alpha P^+, & \hat{\rho}\hat{a} &= \left(\alpha - \frac{\partial}{\partial \alpha^+}\right) P^+, \\ \hat{\rho}\hat{a}^\dagger &= P^+\alpha^+, & \hat{a}^\dagger\hat{\rho} &= \left(\alpha^+ - \frac{\partial}{\partial \alpha}\right) P^+, \end{aligned} \tag{3.21}$$

and

$$
\begin{aligned}
\hat{a}\hat{\rho} &= \left(\alpha + \frac{1}{2}\frac{\partial}{\partial\alpha^*}\right)W, &\qquad \hat{\rho}\hat{a} &= \left(\alpha - \frac{1}{2}\frac{\partial}{\partial\alpha^*}\right)W, \\
\hat{\rho}\hat{a}^\dagger &= \left(\alpha^* + \frac{1}{2}\frac{\partial}{\partial\alpha}\right)W, &\qquad \hat{a}^\dagger\hat{\rho} &= \left(\alpha^* - \frac{1}{2}\frac{\partial}{\partial\alpha}\right)W.
\end{aligned} \tag{3.22}
$$

Direct substitution of these mappings give us the differential equations for each representation.

4 Fokker-Planck equation and stochastic differential equations

"Science cannot solve the ultimate mystery of nature. And that is because, in the last analysis, we ourselves are a part of the mystery that we are trying to solve."

Max Planck 1858-1947

The probability quasidistributions we have discussed so far, are not restricted to behave as an actual probability distribution. However, many times they do. Therefore, the study and use of tools of classical statistics must not scape of our scope. A powerful tool is the so known Fokker-Planck (F-P) equation. Before we show how we connect quasidistributions with the F-P equation, we shall explain what actually a F-P equation is. In order to achieve such a task, we must explain some definitions [73, 74].

Random Variable

Lets define Ω as a set of possible outcomes from a measurable space E. Then a random variable X is a measurable function such that $X : \Omega \to E$. Thus, the probability that an event takes place is given by:

$$Pr(X \in S) = P(\omega \in \Omega | X(\omega) \in E), \tag{4.1}$$

where P is the probability measure.

Markov Process

Lets consider a conditional density probability $P(\vec{x}, t)$, which depends on n random variables such that $\vec{x} = x_1, ..., x_n$. When it is sufficient to know $P(\vec{x_o}, t_o)$, at some $\vec{x}_o$ and t_o in order to know $P(\vec{x}, t)$ at any future time, it is said that the process has the Markov property.

Fokker-Planck equation

A conditional density probability $P(\vec{x}, t|\vec{x_o}, t_o)$, which behaves as a Markov process, usually satisfies the following equation, named as Fokker-Planck equation [74, 75]:

$$\frac{dP(\vec{x}, t|\vec{x_o}, t_o)}{dt} = \left[-\sum_i \frac{\partial}{\partial x_i} A_i(\vec{x}) + \frac{1}{2} \sum_i \sum_j \frac{\partial^2}{\partial x_i \partial x_j} D_{ij}(\vec{x}) \right] P(\vec{x}, t|\vec{x_o}, t_o). \quad (4.2)$$

Here $A_i(\vec{x})$ is known as the drift term and $D_{ij}(\vec{x})$ the diffusion term. Important is to stress the fact that matrix $D_{ij}(\vec{x})$ is symmetric and positive semidefinite.

From the FP equation, we can study the behavior of an ensemble during the time. The average quantities of an observable are calculated as the observable weighted with $P(\vec{x}, t|\vec{x_o}, t_o)$. However, there is also the option to take a different approach. As we have said above $\vec{x}$ is a vector of random variables. For those random variables, we can obtain a set of stochastic differential equations (SDE). The solution of those SDE are single trajectories, which change for any time that are solved. Such that, the average of these trajectories at time t, give us the ensemble's behavior. The corresponding set of SDE, in the Itô approach, which we shall explain later, is given by [74, 73]:

$$\frac{dx_i}{dt} = A_i(\vec{x}) + B_i^j(\vec{x})\xi_j, \quad (4.3)$$

where $D = BB^T$ and ξ_j are δ-correlated Gaussian noise terms, i.e., $\left\langle \overline{\xi_i(t')\xi_j(t)} \right\rangle = \delta_{ij}\delta(t - t')$.

Hence, expectation values are calculated as averages over a large amount of different trajectories generated by Eq. (4.3). The main idea is, once we have the set of SDE, we solved for the initial conditions and generate a great amount of trajectories. When we average all the trajectories, we would have the mean behavior of the ensemble. Such that, without the necessity of solving the F-P type equation, we can study the dynamics of our system of interest.

In order to illustrate the method we show the following example:

Lets consider a F-P equation in one dimension:

$$\frac{dP}{dt} = \left[-\frac{\partial}{\partial x} x + \frac{1}{2} \frac{\partial^2}{\partial x^2} \right] P. \quad (4.4)$$

Following the proceeding described above, the correspondent SDE is:

$$\frac{dx}{dt} = x + \xi. \quad (4.5)$$

By solving numerically Eq. (4.5), several trajectories will be generated. Therefore, it is necessary to solve this equation for several times and take an average over the whole set of trajectories.

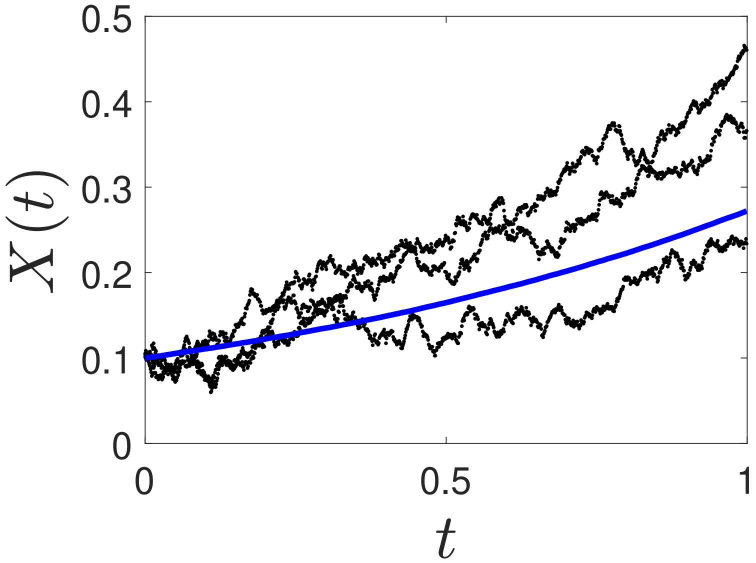

Figure 4.1: Time evolution of x(t). In black there are showed some individual trajectories and in blue it is showed the final average of the trajectories.

In Fig. (4.1), an example of some of the individual trajectories is shown and also the mean behavior. In order to obtain the mean behavior we had to solve Eq. (4.5) 100,000 times.

On the other hand, Eq. (4.4) can be solved quite easy since after applying variable separation such that, if $P(x,t) = P_x(x)P_t(t)$ then P_x satisfies:

$$\left(\frac{\partial^2}{\partial x^2} - 2x\frac{\partial}{\partial x}\right) P_x = (\lambda - 1)P_x, \tag{4.6}$$

where λ is the constant of separation. The solution of Eq. (4.6) are the Hermite polynomials. Thus, for this case there was no need to apply the formalism of SDE. However, for many problems in quantum optics, finding the solutions of F-P equations are not that straightforward, which is the case of the systems treated in this thesis. Therefore, for those problems we must use the SDE formalism.

4.1 Calculus in stochastic processes

In order to treat systems with a stochastic component, an extension of usual calculus is necessary. This extension has two main different approaches: The Itô calculus (which is the one used in this thesis) and the Stratonovich calculus.

Both approaches describe stochastic processes, however, they are not equal. The most immediate (and maybe the most important) difference is the chain rule. While in the Stratonovich calculus the chain rule is the same than in usual calculus, in the Itô calculus it is not. Lets illustrate this.

Itô's formula:

Lets $\vec{x}(t)$ be a vector of random variables. An arbitrary, but twice continuously differentiable, function $f[\vec{x}(t)]$ obeys [73]:

$$\begin{aligned} \frac{df[x(t)]}{dt} &= \sum_i A_i(\vec{x},t)\partial_i f(\vec{x}) + \frac{1}{2}\sum_{i,j}[\boldsymbol{B}(\vec{x},t),\boldsymbol{B^T}(\vec{x},t)]_{ij}\partial_i\partial_j f(\vec{x}) \\ &+ \sum_{i,j} B_{ij}(\vec{x},t)\partial_i f(\vec{x})d\xi_j. \end{aligned} \tag{4.7}$$

This last formula illustrates the fact than in Itô calculus changing variables cannot be done, in general, as in usual calculus. This turns into a difference in the SDE between both approaches, while in the Itô approach is the one showed in (4.3), and in the Stratonovich approach is:

$$\frac{dx_i}{dt} = A_i^{Strat}(\vec{x}) + B_i^j(\vec{x})\xi_j, \tag{4.8}$$

where,

$$A_i^{Strat}(\vec{x}) = A_i(\vec{x}) - \frac{1}{2}\sum_{k,j=1} B_{kj}(\vec{x})\frac{\partial}{\partial x_j}B_{ij}(\vec{x}). \tag{4.9}$$

Eqs.(4.3) and (4.8) reproduce the same results, thus the use of one or the other is a matter of taste.

5 Nonlinear optics

"Nobody ever figures out what life is all about, and it doesn't matter. Explore the world. Nearly everything is really interesting if you go into it deeply enough."

Richard Feynman 1918-1980

The interaction of an electric field with a medium produce an effect of polarization, i.e., the molecules of the medium form dipoles aligned with the electric field. If the electromagnetic field oscillates in the form of a wave, then the formed dipoles oscillate with the frequency of the electromagnetic field. The oscillation of these charges produce radiation as the classical electromagnetic theory predicts. Most of the times, it is said that this polarization it is just proportional to the strength of the electric field applied. However, when the intensity of the electromagnetic wave is high enough, the polarization must be expanded in the following form [76]:

$$\tilde{P}(t) = \epsilon_o \sum_{i=1}^{\infty} \chi^{(i)} \tilde{E}^{(i)}, \tag{5.1}$$

Here $\tilde{E}$ is the electric field, $\tilde{P}$ is the polarization of the medium, ϵ_o is the permissibility of vacuum and $\chi^{(i)}$ are the nonlinear optical susceptibilities of order i which, mathematically, are tensors of rank $i + 1$.

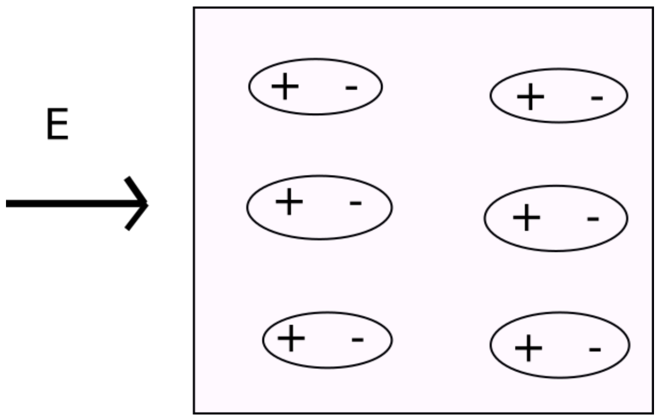

Figure 5.1: Alignment of electric dipoles in a medium due to an applied electric field.

This new expansion allows a great variety of effects which are studied in the so-called field of nonlinear optics. These effects have awake a great interest for both scientific and technology progress since its first observation [77, 78, 79, 76, 80, 81].

In order to illustrate the new effects that can be observed lets consider the following equation derived from Maxwell's equations:

$$\nabla^2 \tilde{E} - \frac{\eta^2}{c^2}\frac{\partial^2 \tilde{E}}{\partial t^2} = \frac{1}{\epsilon_o c^2}\frac{\partial^2 \tilde{P}^{NL}}{\partial t^2}, \tag{5.2}$$

where η is the refractive index, c is the speed of light in vacuum and $\tilde{P}^{NL}$ the nonlinear polarization. Then, if $\tilde{P}^{NL}$ oscillates with frequency ω it would became a source of new radiation with frequency ω.

To illustrate it we shall show the following example:

Second harmonic, sum and difference frequency generation

Lets assume two electromagnetic waves interacting with a non-linear medium with $\chi^{(2)} \neq 0$. The electromagnetic field can be represented as:

$$\tilde{E} = E_1 e^{-i\omega_1 t} + E_2 e^{-i\omega_2 t} + c.c. \tag{5.3}$$

where $\omega_{1,2}$ are optical frequencies that might be, or not, different.

Then, from Eq. (5.1), the second order contribution can be written as:

$$\begin{aligned} \tilde{P}^{(2)} &= \epsilon_o \chi^{(2)} \tilde{E}^{(2)} \\ &= \epsilon_o \chi^{(2)} (E_1^2 e^{-i2\omega_1 t} + E_2^2 e^{-i2\omega_2 t} + 2E_1 E_2 e^{-i(\omega_1+\omega_2)t}) \\ &+ 2E_1 E_2^* e^{-i(\omega_1-\omega_2)t} + c.c. + E_1 E_1^* + E_2 E_2^*. \end{aligned} \tag{5.4}$$

Thus, analyzing the terms on Eq. (5.4) we might obtain all the oscillating terms for the polarization. Here, terms with frequencies $\omega_1 + \omega_2$ and $\pm(\omega_1 - \omega_2)$ correspond to the processes of sum and difference frequency generation, respectively and $2\omega_i$ the generation of second harmonic.

The nonlinear optics is not restricted to second order nonlinear interactions but to any order. However, as we go further in the interaction's order the susceptibility decreases and, therefore, the amplitude of the incident wave must be greater in order to observe the effect. As an example from [76], if $\chi^{(1)} \approx 1$,then $\chi^{(2)} \approx 1.94x10^{-12} m/V$ and $\chi^{(3)} \approx 3.78x10^{-24} m^2/V^2$.

In figure 5.2 it is showed a process of third harmonic generation. As it can be seen, the energy of the generated photons is equal to the incident photons energy. This

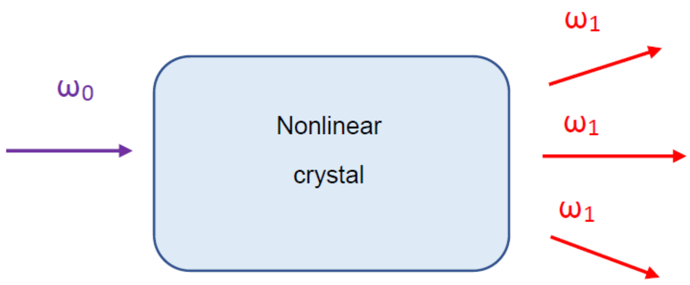

(a) Third harmonic generation.

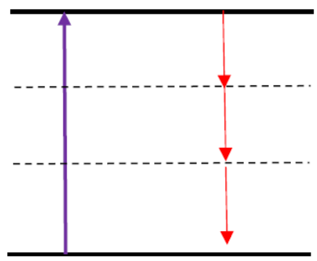

(b) Energy diagram.

Figure 5.2: a) Representation of a process of third harmonic generation in a nonlinear crystal. b) Energy diagram for third harmonic generation.

lead us to a essential part in the nonlinear optics; the phase-matching conditions. In order to obtain an efficient process there are two conditions that must be fulfilled:

$$\sum_i \omega_i^{(p)} = \sum_n \omega_n^{(o)}, \tag{5.5}$$

$$\sum_i \vec{k}_i^{(p)} = \sum_n \vec{k_n}^{(o)}, \tag{5.6}$$

where $\omega^{(p)}(\omega^{(o)})$ are the frequencies of the incident (output) light and $\vec{k}^{(p)}(\vec{k}^{(o)})$ the wave number vector. Both conditions are no more but conditions of conservation of energy and linear momentum respectively. If Eq.(5.6) is not fulfilled perfectly, but the difference is small it is said that the waves are quasi phase-matched. This may occur by different reasons, from the experimental set up to the dispersion in the medium. The importance of phase-matching lay in the fact that the greater the miss-matching the lower the efficiency of the process. This was first showed by Maker [78], where it is showed that varying the angle of incidence of the light in the crystal the efficiency varies abruptly.

6 Physical Model

"Mathematics is only a tool and one should learn to hold the physical ideas in one's mind without reference to the mathematical form."

Paul A.M. Dirac 1902-1984

So far we have discussed the preliminary subjects for this thesis' work. Now we shall discuss the model that we studied.

Our goal is to find a platform where three entangled modes of the electromagnetic field (photons) can be generated. There have been many proposals of how to generate such states as we have mentioned before. Here we focus on generation of bipartite and multipartite entangled states by using a third-order non-linear interaction. We will take different approaches to the problem, i.e., different interaction Hamiltonians, in order to study quantum correlations between different parts of the system.

6.1 Hamiltonians

Firstly, we consider the case in which there are only two type of modes, high ω_p and low ω_o frequency, such that $\omega_p = 3\omega_o$. The first Hamiltonian that we consider is denoted by $\hat{H}^{(1)}$, and corresponds to:

$$\hat{H}^{(1)} = \frac{i\hbar\kappa}{3}\left[\hat{b}\hat{a}^{\dagger 3} - \hat{b}^{\dagger}\hat{a}^{3}\right], \tag{6.1}$$

where $\hat{b}$ ($\hat{a}$) is the annihilation operator for ω_p (ω_o) mode and κ is the effective nonlinear coupling between the nonlinear medium and the pump beam. Throughout this thesis we will take $\hbar = 1$. This Hamiltonian corresponds to the degenerate case. There are two processes which can be described by this Hamiltonian, which are third harmonic generation (THG) and three-photon-down-conversion (TPDC).

In order to obtain a more general Hamiltonian we separate *step by step* the low-frequency modes. Thus, separating one low-frequency mode such that $\hat{a}^3 \to \hat{a}_1^2\hat{a}_3$ we get the following Hamiltonian, denoted by $\hat{H}^{(2)}$:

$$\hat{H}^{(2)} = i\hbar\kappa\left[\hat{b}\hat{a}_1^{\dagger 2}\hat{a}_3^{\dagger} - \hat{b}^{\dagger}\hat{a}_1^{2}\hat{a}_3\right], \tag{6.2}$$

here $\hat{a}_1$ ($\hat{a}_3$) is the annihilation operator for the ω_1 (ω_3) mode, where $\omega_p = 2\omega_1 + \omega_3$.

Finally, separating all low-frequency modes which is made by taking $\hat{a}^3 \to \hat{a}_1\hat{a}_2\hat{a}_3$, we get that the Hamiltonian, denoted by $\hat{H}^{(3)}$ is:

$$\hat{H}^{(3)} = i\hbar\kappa \left[\hat{b}\hat{a}_1^\dagger\hat{a}_2^\dagger\hat{a}_3^\dagger - \hat{b}^\dagger\hat{a}_1\hat{a}_2\hat{a}_3\right], \tag{6.3}$$

where $\hat{a}_i$ is the annihilation operator for the ω_i mode and $\omega_p = \omega_1 + \omega_2 + \omega_3$.

These three interaction Hamiltonians describe either a three-photon-down-conversion (TPDC) or a Sum frequency generation (SFG) process. Since the analytic solutions of Eq. (3.20) for these Hamiltonians are not easy to find we use standard methods for quantum optics [63].

These methods map the time evolution of the density operator to a set of SDE, as discussed in section (3.3).Below we show this procedure, obtaining the corresponding SDE for both the positive-P and Wigner functions, for the different Hamiltonians discussed above.

6.1.1 Positive P function approach

Using Eq. (3.20) and mappings (3.21) we obtain the following time evolution equation for the positive-P function for $\hat{H}^{(1)}$:

$$\begin{aligned}\frac{\partial}{\partial t}P^{(1)} &= \kappa\left[-\frac{\partial}{\partial\alpha}(\alpha^{+^2}\beta) - \frac{\partial}{\partial\alpha^+}(\alpha^2\beta^+) + \frac{\partial}{\partial\beta}\left(\frac{\alpha^3}{3}\right)\right.\\ &+ \frac{\partial}{\partial\beta^+}\left(\frac{\alpha^{+3}}{3}\right) + \frac{1}{2}\frac{\partial^2}{\partial\alpha^2}(2\alpha^+\beta) + \frac{1}{2}\frac{\partial^2}{\partial\alpha^{+2}}(2\alpha\beta^+)\\ &- \left.\frac{1}{6}\left(\frac{\partial^3}{\partial\alpha^3}(2\beta) + \frac{\partial^3}{\partial\alpha^{+3}}(2\beta^+)\right)\right]P^{(1)}.\end{aligned} \tag{6.4}$$

It is important to note that α^+ is not the complex conjugate of α, in fact they are different variables. Nevertheless, over a large number of trajectories they both behave as complex conjugates.

It is easy to realize that if there were no third-order derivatives, the time evolution differential equation would be a Fokker-Planck type equation. Such that, we would be able to map this equation directly to a set of SDE. Thus, in order to do so, we must make some considerations: Firstly, at $t = 0$, we may say each mode is in a coherent state, $|\alpha_o\rangle$ and $|\beta_o\rangle$, for ω_o and ω_p respectively. Therefore, $P^{(1)}(t = 0) = \delta(\alpha - \alpha_o)\delta(\alpha^+ - \alpha_o^+)\delta(\beta - \beta_o)\delta(\beta^+ - \beta_o^+)$. In the case of SFG (third harmonic generation since all low-frequency modes have frequency ω_o) $\beta_o = \beta_o^* = 0$. Thus, at this time third order derivatives vanish. For a time scale where the influence of third order derivatives is negligible, we can map the resulting FP to a set of SDE.

This set corresponds to:

$$
\begin{aligned}
d\alpha &= \kappa\alpha^{+2}\beta dt + \sqrt{2\kappa\alpha^{+}\beta}d\xi_1(t), \\
d\alpha^{+} &= \kappa\alpha^{2}\beta dt + \sqrt{2\kappa\alpha\beta^{+}}d\xi_2(t), \\
d\beta &= -\frac{\kappa}{3}\alpha^{3}dt, \\
d\beta^{+} &= -\frac{\kappa}{3}\alpha^{+3}dt,
\end{aligned}
\tag{6.5}
$$

Solving these equations numerically over a large number of trajectories, allows us to calculate all the required expectation values for the witnesses described in Section (2.3). Following a similar procedure for $\hat{H}^{(2)}$ and $\hat{H}^{(3)}$, we obtain their corresponding set of SDE. These are for $\hat{H}^{(2)}$:

$$
\begin{aligned}
d\alpha_1 &= (2\kappa\alpha_1^{+}\alpha_3^{+})dt - 2\sqrt{i\alpha_3^{+}\beta}d\xi_{13}^{*}, \\
d\alpha_3 &= (\kappa\alpha_1^{+2})dt + \sqrt{\frac{i\alpha_1^{+2}\beta}{\alpha_3^{+}}}id\xi_{13}, \\
d\alpha_1^{+} &= (2\kappa\alpha_2\alpha_3)dt - \sqrt{i\alpha_3\beta^{+}}d\xi_{13}^{+*}, \\
d\alpha_3^{+} &= (\kappa\alpha_1\alpha_2)dt + \sqrt{\frac{i\alpha_1^{2}\beta^{+}}{\alpha_3}}id\xi_{13}^{+}, \\
d\beta^{+} &= -\alpha_1^{+2}\alpha_3^{+}dt, \\
d\beta &= -\alpha_1^{2}\alpha_3 dt.
\end{aligned}
\tag{6.6}
$$

while for $\hat{H}^{(3)}$:

$$
\begin{aligned}
d\alpha_1 &= (\kappa\alpha_2^{+}\alpha_3^{+})dt + \sqrt{\frac{i\alpha_2^{+}\alpha_3^{+}\beta}{\alpha_1^{+}}}(-id\xi_{12}^{*} - d\xi_{13}^{*}), \\
d\alpha_2 &= (\kappa\alpha_1^{+}\alpha_3^{+})dt + \sqrt{\frac{i\alpha_3^{+}\alpha_1^{+}\beta}{\alpha_2^{+}}}(-d\xi_{12} + id\xi_{23}^{*}), \\
d\alpha_3 &= (\kappa\alpha_1^{+}\alpha_2^{+})dt + \sqrt{\frac{i\alpha_1^{+}\alpha_2^{+}\beta}{\alpha_3^{+}}}(id\xi_{13} + d\xi_{23}), \\
d\alpha_1^{+} &= (\kappa\alpha_2\alpha_3)dt + \sqrt{\frac{i\alpha_2\alpha_3\beta^{+}}{\alpha_1}}(-id\xi_{12}^{+*} - d\xi_{13}^{+*}), \\
d\alpha_2^{+} &= (\kappa\alpha_1\alpha_3)dt + \sqrt{\frac{i\alpha_1\alpha_3\beta^{+}}{\alpha_2}}(-d\xi_{12}^{+} + id\xi_{23}^{+*}), \\
d\alpha_3^{+} &= (\kappa\alpha_1\alpha_2)dt + \sqrt{\frac{i\alpha_1\alpha_2\beta^{+}}{\alpha_3}}(id\xi_{13}^{+} + d\xi_{23}^{+}), \\
d\beta^{+} &= -\alpha_1^{+}\alpha_2^{+}\alpha_3^{+}dt, \\
d\beta &= -\alpha_1\alpha_2\alpha_3 dt.
\end{aligned}
\tag{6.7}
$$

6.1.2 Wigner function

In this section we show the set of SDE using the Wigner function for the different cases under study. These will allow us to compare the results of both representations, which are the positive-P and the Wigner function.

For $H^{(1)}$, the differential equation for the Wigner representation is:

$$\begin{aligned}\frac{\partial}{\partial t}W^{(1)} &= \frac{\kappa}{3}\left[(\beta+\frac{1}{2}\frac{\partial}{\partial\beta^*})(\alpha^*-\frac{1}{2}\frac{\partial}{\partial\alpha})^3\right]W^{(1)} \\ &- \frac{\kappa}{3}\left[(\beta-\frac{1}{2}\frac{\partial}{\partial\beta^*})(\alpha^*+\frac{1}{2}\frac{\partial}{\partial\alpha})^3\right]W^{(1)} \\ &+ C.C. \end{aligned} \tag{6.8}$$

We now take the well-known truncated Wigner approximation, in order to drop third order derivatives terms. This allow us to find the following differential coupled equations:

$$\begin{aligned}\frac{d\alpha}{dt} &= \kappa\alpha^{*2}\beta, \\ \frac{d\beta}{dt} &= -\frac{\kappa}{3}\alpha^3.\end{aligned}$$

The first thing to realize about these equations is that they do not have an explicit noise term. However, the fluctuations are due to the initial conditions. The Wigner function at $t=0$ is: $W(t=0)=\frac{4}{\pi^2}\exp(-2|\alpha-\alpha_o|^2-2|\beta-\beta_o|^2)$. Hence, the initial conditions are given by a Gaussian distribution. Such that, for any single trajectory the initial conditions will not be the same.

Similarly, for $\hat{H}^{(2)}$ we find the following set of equations:

$$\begin{aligned}\frac{d\alpha_1}{dt} &= 2\kappa\alpha_1^*\alpha_3^*\beta, \\ \frac{d\alpha_3}{dt} &= \kappa\alpha_1^{*2}\beta, \\ \frac{d\beta}{dt} &= -\kappa\alpha_1^2\alpha_3,\end{aligned} \tag{6.9}$$

and for $\hat{H}^{(3)}$ the set is:

$$\begin{aligned} \frac{d\alpha_1}{dt} &= \kappa\alpha_2^*\alpha_3^*\beta, \\ \frac{d\alpha_2}{dt} &= \kappa\alpha_1^*\alpha_3^*\beta, \\ \frac{d\alpha_3}{dt} &= \kappa\alpha_1^*\alpha_2^*\beta, \\ \frac{d\beta}{dt} &= -\kappa\alpha_1\alpha_2\alpha_3. \end{aligned} \tag{6.10}$$

6.1.3 Numerical method

In order to solve the last sets of SDE we used the method of central difference. This method is explained below.

Lets consider a first order differential equation with the form $y' = f(t, y)$. If we know $y(0)$ and, on taking $y(0) = y_0$, we can make finite differences such that:

$$k_1 = hf(t_n, y_n), \tag{6.11}$$

$$k_2 = hf(t_n + \frac{h}{2}, y_n + \frac{k_1}{2}), \tag{6.12}$$

$$k_3 = hf(t_n + \frac{h}{2}, y_n + \frac{k_2}{2}), \tag{6.13}$$

thus the solution y_{n+1} is:

$$y_{n+1} = y_n + k_3 + O(h^3). \tag{6.14}$$

As we can see the error of this method is of order h^3. In that way we can numerically solve the set of SDE.

6.1.4 Example of method

In order to illustrate how phase-space methods are implemented, we will illustrate with the following example using the positive-P representation. To this end, lets consider the following Hamiltonian:

$$\hat{H} = \hbar\kappa(\hat{a}_1^\dagger\hat{a}_2^\dagger\hat{a}_3^\dagger + \hat{a}_1\hat{a}_2\hat{a}_3). \tag{6.15}$$

This Hamiltonian is the Hamiltonian $H^{(3)}$ under the undepleted approach. Now, lets consider that one mode behaves as a classical one. Such that $\hat{a}_3 = iE_3$, thus the Hamiltonian of Eq. (6.15) becomes:

$$\hat{H}_2 = i\kappa E_3(\hat{a}_1\hat{a}_2 - \hat{a}_1^\dagger\hat{a}_2^\dagger). \tag{6.16}$$

For this case, on taking $\kappa E_3 \to \kappa$, analytical solutions for the operators $\hat{a}_{1,2}$ in the Heisenberg approach can be obtained as:

$$\begin{aligned}\hat{a}_1 &= \hat{a}_1 \cosh(\kappa t) - \frac{\kappa}{|\kappa|}\hat{a}_2^\dagger \sinh(\kappa t),\\ \hat{a}_2 &= \hat{a}_2 \cosh(\kappa t) - \frac{\kappa}{|\kappa|}\hat{a}_1^\dagger \sinh(\kappa t),\end{aligned} \tag{6.17}$$

Using the criteria of Duan et al (2.4), and assuming that the initial state is the vacuum, we find that a violation of the following inequality certifies bipartite entanglement:

$$\Delta^- = 4(\cosh^2(|\kappa|t) + \sinh^2(|\kappa|t) - \left(\frac{\kappa^*}{|\kappa|} + \frac{\kappa}{|\kappa|}\right)\cosh(|\kappa|t)\sinh(|\kappa|t)) > 4. \tag{6.18}$$

even more the evolution of the expectation value of the number operator for each modes, is:

$$\left\langle \hat{a}_i^\dagger \hat{a}_i \right\rangle = \sinh^2(t), \qquad i = 1, 2. \tag{6.19}$$

Now, the differential equation for the positive-P representation is given by:

$$\begin{aligned}\frac{dP}{dt} &= \kappa\Bigg[\alpha_1\alpha_2 - \left(\alpha_1^+ - \frac{\partial}{\partial\alpha_1}\right)\left(\alpha_2^+ - \frac{\partial}{\partial\alpha_2}\right)\\ &- \left(\alpha_1 - \frac{\partial}{\partial\alpha_1^+}\right)\left(\alpha_2 - \frac{\partial}{\partial\alpha_2^+}\right) + \alpha_1^+\alpha_2^+\Bigg]P.\end{aligned} \tag{6.20}$$

The diffusion matrix, D, for this F-P type equation is:

$$D = \begin{bmatrix} 0 & \kappa & 0 & 0\\ \kappa & 0 & 0 & 0\\ 0 & 0 & 0 & \kappa\\ 0 & 0 & \kappa & 0 \end{bmatrix}, \tag{6.21}$$

and its factorization B is:

$$B = -i\begin{bmatrix} 0 & \sqrt{\kappa} & 0 & 0\\ \sqrt{\kappa} & 0 & 0 & 0\\ 0 & 0 & 0 & \sqrt{\kappa}\\ 0 & 0 & \sqrt{\kappa} & 0 \end{bmatrix}. \tag{6.22}$$

Therefore, following the technique explained in chapter 4, this equation can be mapped to the following set of SDE:

$$\begin{aligned}d\alpha_1 &= -\kappa\alpha_2^+ dt - i\sqrt{\kappa}dW_1,\\ d\alpha_2 &= -\kappa\alpha_1^+ dt - i\sqrt{\kappa}dW_1^+,\\ d\alpha_1^+ &= -\kappa\alpha_2 dt - i\sqrt{\kappa}dW_2,\\ d\alpha_2^+ &= -\kappa\alpha_1 dt - i\sqrt{\kappa}dW_2^+.\end{aligned} \tag{6.23}$$

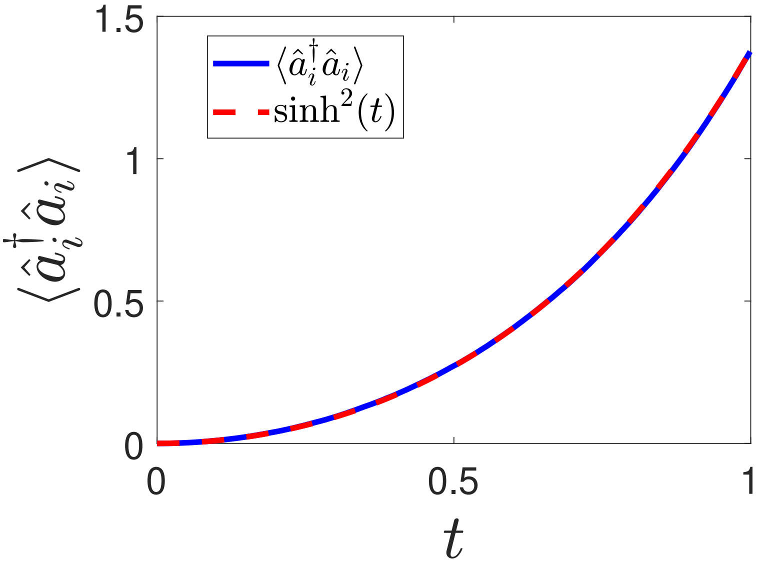

Figure 6.1: Time evolution for the number operator using analytical and numerical solutions

We now shall show the solutions for $\left\langle \hat{a}_i^\dagger \hat{a}_i \right\rangle$ and Δ^- using Eqs. (6.23) and the analytical solutions given in Eqs. (6.18) and (6.19).

As we can see from figures (6.1) and (6.2) the numerical solutions for the set of SDE obtained for the positive-P representation, either for the witness or the number operator, are in a good agreement with the analytical ones.

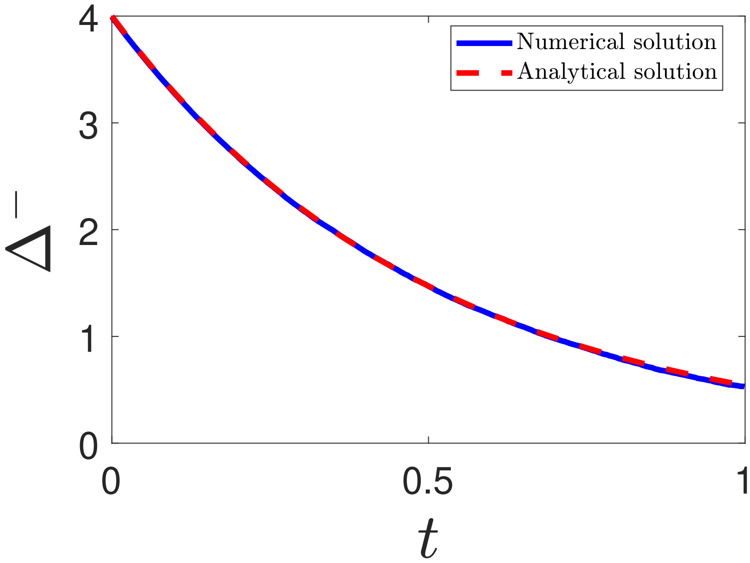

Figure 6.2: Time evolution of Duan witnessing using analytical and numerical solution

7 Results

"It seems to me a fundamental dishonesty, and a fundamental treachery to intellectual integrity to hold a belief because you think it's useful and not because you think it's true."

Bertrand Russell 1872-1970

In this Chapter, we show the results for the time evolution of the system under study for all the different Hamiltonians that were described previously. This will be done in the following way. First, we discuss the results for $\hat{H}^{(1)}$, i.e., all the low-frequency modes are included in one mode. Then, we explain the case of Hamiltonian $\hat{H}^{(2)}$, where one low-frequency mode was separated for the other two. This means that two low-frequency modes remain in one mode. At the end, we treat the Hamiltonian $\hat{H}^{(3)}$. As we have mentioned previously, this last Hamiltonian represents the most general one of the three under consideration. Following this procedure, we ensure the study of entanglement and steering between modes in any composite or individual subsystem by using different approaches.

For all these cases, we numerically solve all the different set of SDE, using both representations the positive-P and the Wigner one. These numerical simulations were performed over 3×10^5 stochastic trajectories, with $\kappa = 10^{-3}$.

Even though, most of the results for $\hat{H}^{(1)}$ were already reported by Olsen in [48], using only the positive-P function, we go further by using both phase-space representations and on studying the dynamics of the Ent^- witness. As we will see, the addition of that witness will show some significant results.

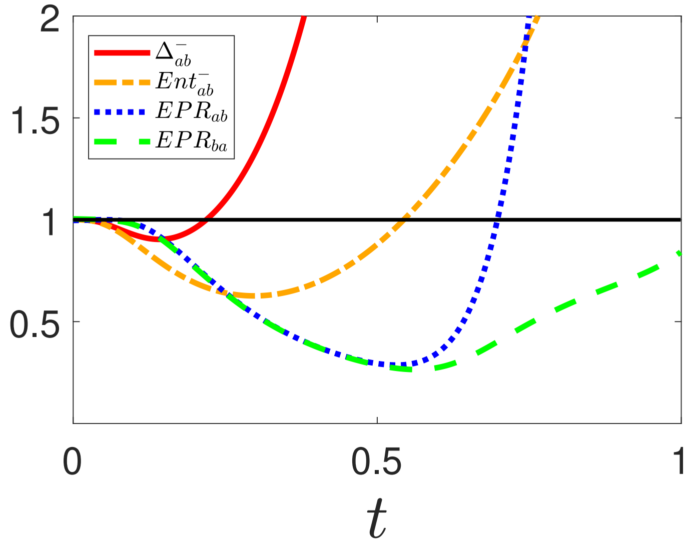

Figure 7.1: Bipartite correlations for third-harmonic generation using $\hat{H}^{(1)}$. Here $|\langle\alpha(0)\rangle = 10^4|$ and the witnesses $\Delta^{\pm}$ and $Ent^{\pm}$ were normalized, so that the bound of the inequalities coincide with the one of EPR_{ab} (EPR_{ba}).

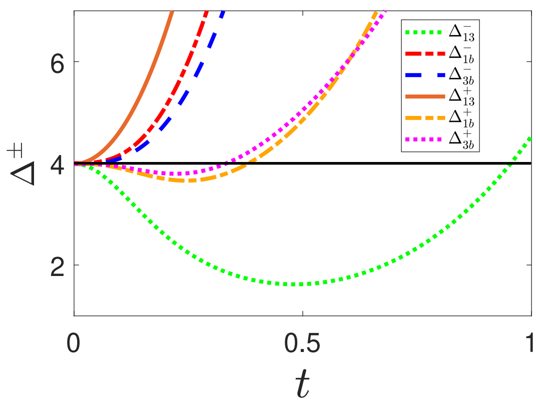

(a) $\Delta^{\pm}$ criterion.

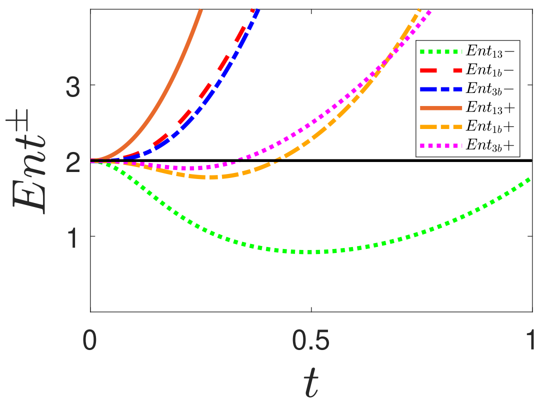

(b) $Ent^{\pm}$ criterion.

Figure 7.2: Bipartite entanglement witnesses for SFG using $\hat{H}^{(2)}$. (a) $\Delta^{\pm}$ criterion. (b) $Ent^{\pm}$ criterion. Here $|\langle\alpha_1(0)\rangle = 10^4|$ and $|\langle\alpha_3(0)\rangle = 10^4/3|$.

In Fig. 7.1 the time evolution of the entanglement (Δ^- and Ent^-) and the steering (EPR) bipartite witnesses are showed. We observe that both modes, $\hat{b}$ and $\hat{a}$, are entangled and even more they are steerable by each other. These results were showed by Olsen in [48], using only the positive-P representation and the DGCZ entanglement criteria Δ^-. As we said above, in this thesis we performed the numerical simulations using both phase-space representations which are the Wigner

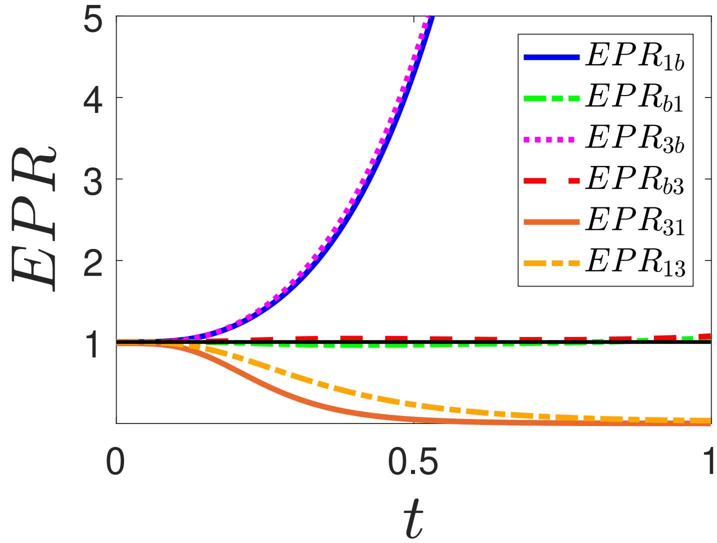

Figure 7.3: Bipartite steering criterion for SFG using $\hat{H}^{(2)}$. Here $|\langle\alpha_1(0)\rangle = 10^4|$ and $|\langle\alpha_3(0)\rangle = 10^4/3|$.

and positive-P function, We also considered the entanglement criterion Ent as well. However, since the results for both representations were the same, here we only show the results obtained with the Wigner function. The addition of Ent^- showed us that this witness is more robust to certify quantum entanglement than $\Delta^\pm$ for this system.

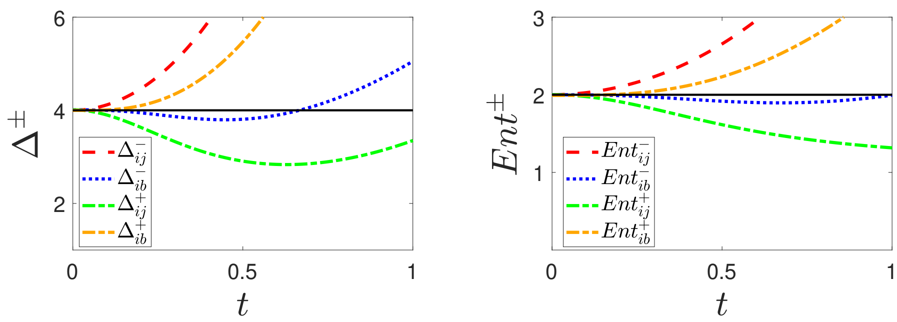

(a) $\Delta^\pm$ criterion **(b)** $Ent^\pm$ criterion

Figure 7.4: Entanglement bipartite witness for SFG using $\hat{H}^{(3)}$. Here $|\langle\alpha_i(0)\rangle = 10^4/3|$ and $i = 1, 2, 3$.

In Fig. 7.2, the bipartite entanglement witnesses for $\hat{H}^{(2)}$ is shown. As a first result, we obtain that all possible combinations of bipartite entanglement between modes are present. Nevertheless, entanglement witnessing between modes $\hat{a}_1$ and $\hat{a}_3$, is more efficient than witnessing with the mode $\hat{b}$. Once again, $Ent^\pm$ witness certify entanglement longer that $\Delta^{\pm}$. However, we note that both criteria have a qualitatively similar behaviour. In Fig. 7.3 the EPR steering criteria is shown. Here we note that, as a consequence of taking the low frequency modes ($\hat{a}_1$ and $\hat{a}_3$) to be different, we certified two way steering between these two modes. In addition, the steering holds during all the simulation.

In Fig. 7.4 we plot $\Delta^{\pm}$ and $Ent^{\pm}$. Both witnesses certify that all combinations of bipartite entanglement are possible between the different modes of $\hat{H}^{(3)}$. In order to certify bipartite entanglement, we have to consider both combination of signs $\left(g^{(sym)} = \pm 1\right)$, for $\Delta^{\pm}$ and $Ent^{\pm}$. In addition, entanglement between low-frequency modes holds during all the simulation. While entanglement witnessing between modes $\hat{a}_i$ and mode $\hat{b}$ does not hold.

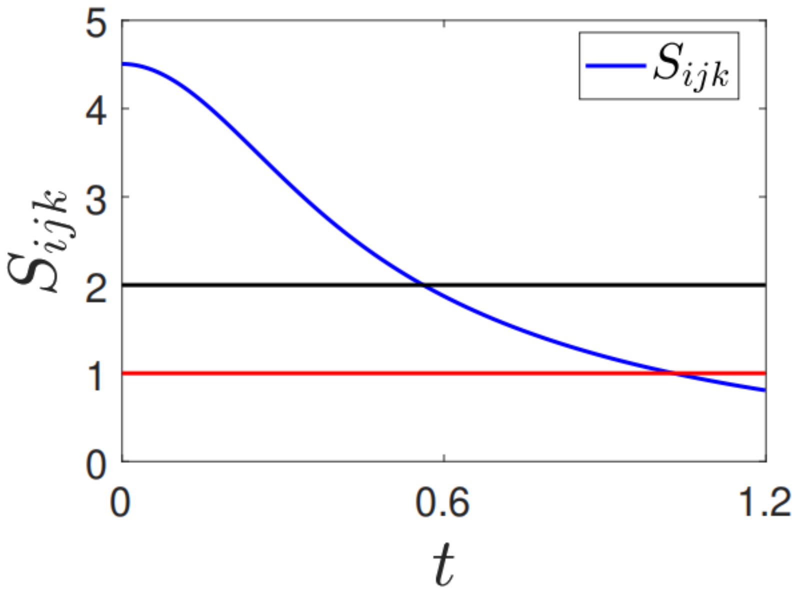

Figure 7.5: Tripartite entanglement and steering for sum frequency generation between low-frequency modes for $\hat{H}^{(3)}$. Here $|\langle \alpha_i(0) \rangle = 10^4/3|$ and $i = 1, 2, 3$

In Fig. 7.5 the time evolution of the tripartite criterion S given in Eq. (2.16) is shown. We can observe that in the process of SFG, tripartite entanglement and steering are generated between the low-frequency modes. In Fig. 7.6 we show the dynamics of bipartite EPR steering and its monogamy relation. In 7.6(a) there is no bipartite steering witnessing between any of the modes, even when tripartite steering is present. The actual meaning of this is that the EPR_{ij} witness is no capable to certify steering for this situation, even if it is present. Using Eq. (2.18) we realized that EPR_{ij} has a lower bound as a result of the monogamy relation as is showed in Fig. 7.6(b). Therefore, it is not possible to certify bipartite steering using this witness. As before, the results are the same with both representations.

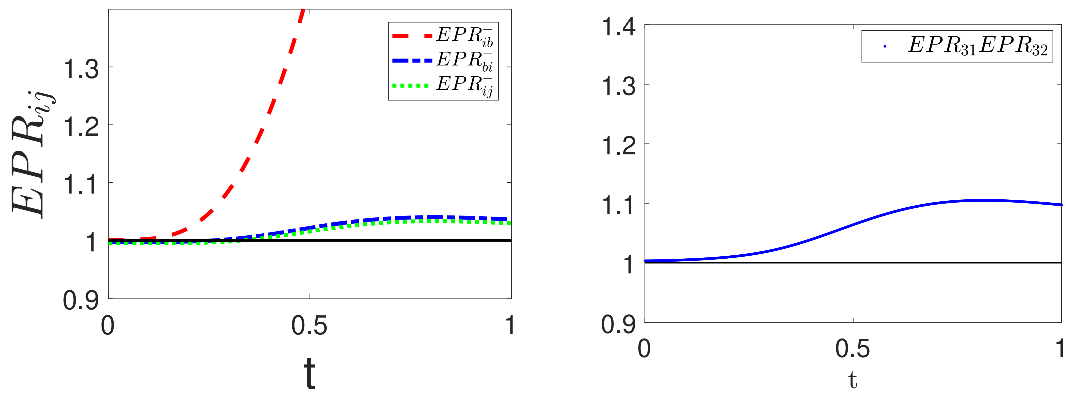

(a) Time evolution for the EPR criterion. **(b)** Time evolution for the monogamy relation.

Figure 7.6: Time evolution for the EPR criterion and its respective monogamy relation for $\hat{H}^{(3)}$.

Finally, we want to prove that the final state of Hamiltonian $H^{(3)}$ is a four parties entangled state. In order to do so we will consider the following results:

Result 1. The tripartite state of all the LF modes is genuinely entangled.

Result 2. The HF mode is entangled in pairs with all the LF modes.

Result 1 implies that the density operator for the LF modes $\hat{\rho}_{123}$ cannot be represented in a biseparable form [82, 83], which is:

$$\begin{aligned} \hat{\rho}_{123} &= \sigma_1 \sum_i \omega_i^1 \hat{\rho}_1^i \otimes \hat{\rho}_{23}^i + \sigma_2 \sum_j \omega_j^2 \hat{\rho}_2^j \otimes \hat{\rho}_{13}^j \\ &+ \sigma_3 \sum_k \omega_k^3 \hat{\rho}_3^k \otimes \hat{\rho}_{12}^k, \end{aligned} \tag{7.1}$$

where $\sum_{i=1}^3 \sigma_i = 1$ and $\sum_j \omega_j^n = 1$, with $n = 1, 2, 3$.

Thus if the LF modes and the HF mode are not a four modes entangled state, then the density operator for the whole system, $\hat{\rho}$, can be expressed as:

$$\hat{\rho} = \sum_j \omega_j \hat{\rho}_H^j \otimes \hat{\rho}_{123}^j. \tag{7.2}$$

Here $\hat{\rho}_H$ is the density operator of the HF mode and $\hat{\rho}_{123}^j$ are the density operators of the tripartite entangled state. However, Result 2 implies that $\hat{\rho}$ cannot be written as Eq. (7.2). Thus, from Result 2 and considering that the LF modes and the HF mode are not a four modes entangled state, the density operator can be written as:

$$\begin{aligned} \hat{\rho} &= \sigma_1 \sum_i \omega_i^1 \hat{\rho}_{H1}^i \otimes \hat{\rho}_{23}^i + \sigma_2 \sum_j \omega_j^2 \hat{\rho}_{H2}^j \otimes \hat{\rho}_{13}^j \\ &+ \sigma_3 \sum_k \omega_k^3 \hat{\rho}_{H3}^k \otimes \hat{\rho}_{12}^k + \sigma_4 \sum_m \omega_m^4 \hat{\rho}_{H12}^m \otimes \hat{\rho}_3^m \\ &+ \sigma_5 \sum_n \omega_n^5 \hat{\rho}_{H13}^n \otimes \hat{\rho}_2^n + \sigma_6 \sum_l \omega_l^6 \hat{\rho}_{H23}^l \otimes \hat{\rho}_1^l. \end{aligned} \tag{7.3}$$

Here $\sum_{i=1}^{6} \sigma_i = 1$, $\hat{\rho}_{ab}^c$, where a and b represents the LF modes, could be the density operators of either entangled or separable states, and $\hat{\rho}_{Ha}^c$ are entangled density operators for the HF mode with the LF modes.

We note that Eq. (7.3) is a biseparable representation of the LF modes. However as we have mentioned above, $\hat{\rho}$ cannot be represented as that. Thus, the only way to satisfy both results is by considering the whole state as an entangled one. Such that the density operator should be written as:

$$\hat{\rho} = \sum_j \omega_j \hat{\rho}_{H123}^j. \tag{7.4}$$

Therefore, we have shown that the four parties are entangled. This type of entanglement is similar to the tripartite state formed by the pump, signal and idler modes obtained at the output of an optical parametric oscillator (OPO) [84].

8 Conclusion

"Let me say it again: You must not come lightly to the blank page."

Stephen King

In this thesis we have studied the capability of a nonlinear optical medium to generate quantum entangled states of light. In order to do this, we have used the quantum approach to the interaction of light with the nonlinear medium. In particular, we have observed that these kind of systems can be studied by using the well-known phase-space methods of quantum optics.

In the results of this thesis, we report that at the output of SFG the three low-frequency modes are entangled and, even more, present tripartite steering. It was necessary to make a distinction between low-frequency ($\hat{a}^3 \rightarrow \hat{a}_1\hat{a}_2\hat{a}_3$) modes in order to certify the creation of this tripartite entangled state. In addition, we concluded that the high-frequency mode is entangled with each of the low-frequency modes and with the composite system of them. Moreover, using these last results we found that the output formed by all the modes form a four modes multicolored entangled state.

Our calculations, showed that, even when third order derivatives where dropped in order to obtain a Fokker-Planck type equation, all results are consistent and, even more, satisfies perfectly the monogamy relation. Curiously, even when we observed that the low-frequency modes are steerable by each other, the witness for bipartite steering was not able to certify it. We conclude this might be due to the monogamy relation and not for a lack of bipartite steering.

Finally, since we have observed that this phenomena has a great variety of correlations at different levels, this thesis provides a new way to generate four entangled multicolored modes and tripartite steerable states in one single experiment.

Bibliography

[1] T. H. Maiman. Stimulated optical radiation in ruby. *Nature*, 3(7):493–494, 1960.

[2] I. M. Ross. The invention of the transistor. *Proceedings of the IEEE*, 86(1):7–28, Jan 1998.

[3] W. P. Schleich et al. Quantum technology: from research to application. *Applied Physics B*, 122:130, 2016.

[4] Antonio Acín, Immanuel Bloch, Harry Buhrman, Tommaso Calarco, Christopher Eichler, Jens Eisert, Daniel Esteve, Nicolas Gisin, Steffen J Glaser, Fedor Jelezko, Stefan Kuhr, Maciej Lewenstein, Max F Riedel, Piet O Schmidt, Rob Thew, Andreas Wallraff, Ian Walmsley, and Frank K Wilhelm. The quantum technologies roadmap: a european community view. *New Journal of Physics*, 20(8):080201, 2018.

[5] Michael A Nielsen and Isaac L Chuang. Quantum computation and quantum information, 2000.

[6] Vittorio Giovannetti, Seth Lloyd, and Lorenzo Maccone. Advances in quantum metrology. *Nature Photonics*, 5:222, 2011.

[7] Vittorio Giovannetti, Seth Lloyd, and Lorenzo Maccone. Quantum-Enhanced Measurements: Beating the Standard Quantum Limit. *Science*, 306(5700):1330–1336, 2004.

[8] Hidehiro Yonezawa, Takao Aoki, and Akira Furusawa. Demonstration of a quantum teleportation network for continuous variables. *Nature*, 431:430–433, 2004.

[9] Daniele Binosi. Quantum manifesto endorsement, 2016.

[10] P. Shor. Polynomial-time algorithms for prime factorization and discrete logarithms on a quantum computer. *SIAM Review*, 41(2):303–332, 1999.

[11] Luigi Amico, Rosario Fazio, Andreas Osterloh, and Vlatko Vedral. Entanglement in many-body systems. *Rev. Mod. Phys.*, 80:517–576, 2008.

[12] Ryszard Horodecki, Paweł Horodecki, Michał Horodecki, and Karol Horodecki. Quantum entanglement. *Rev. Mod. Phys.*, 81:865–942, 2009.

[13] Anton Zeilinger. Light for the quantum. Entangled photons and their applications: a very personal perspective. *Physica Scripta*, 92(7):072501, 2017.

[14] A. Einstein, B. Podolsky, and N. Rosen. Can quantum-mechanical description of physical reality be considered complete? *Phys. Rev.*, 47:777–780, 1935.

[15] E. Schrödinger. Discussion of probability relations between separated systems. *Mathematical Proceedings of the Cambridge Philosophical Society*, 31:555–563, 1935.

[16] J. S. Bell. On the einstein podolsky rosen paradox. *Physics Physique Fizika*, 1:195–200, Nov 1964.

[17] John F. Clauser and Abner Shimony. Bell's theorem. Experimental tests and implications. *Rep. Prog. Phys.*, 41(12):1881–1927, 1978.

[18] Stuart J. Freedman and John F. Clauser. Experimental test of local hidden-variable theories. *Phys. Rev. Lett.*, 28:938–941, Apr 1972.

[19] Alain Aspect, Philippe Grangier, and Gérard Roger. Experimental tests of realistic local theories via bell's theorem. *Phys. Rev. Lett.*, 47:460–463, Aug 1981.

[20] Alain Aspect, Jean Dalibard, and Gérard Roger. Experimental test of bell's inequalities using time-varying analyzers. *Phys. Rev. Lett.*, 49:1804–1807, Dec 1982.

[21] Alain Aspect. Bell's inequality test: more ideal than ever. *Nature*, 398:189–190, 1999.

[22] John F. Clauser. *Bell's Theorem, Bell Inequalities, and the "Probability Normalization Loophole"*, pages 451–484. Springer International Publishing, Cham, 2017.

[23] B Hensen, H Bernien, A E. Dréau, Andreas Reiserer, Norbert Kalb, M S. Blok, J Ruitenberg, R F. L. Vermeulen, R N. Schouten, Carlos Abellan, Waldimar Amaya, V Pruneri, Morgan Mitchell, M Markham, Daniel Twitchen, David Elkouss, S Wehner, Tim Taminiau, and R Hanson. Loophole-free bell inequality violation using electron spins separated by 1.3 kilometres. *Nature*, 526, 10 2015.

[24] Lynden K. Shalm, Evan Meyer-Scott, Bradley G. Christensen, Peter Bierhorst, Michael A. Wayne, Martin J. Stevens, Thomas Gerrits, Scott Glancy, Deny R. Hamel, Michael S. Allman, Kevin J. Coakley, Shellee D. Dyer, Carson Hodge, Adriana E. Lita, Varun B. Verma, Camilla Lambrocco, Edward Tortorici, Alan L. Migdall, Yanbao Zhang, Daniel R. Kumor, William H. Farr, Francesco Marsili, Matthew D. Shaw, Jeffrey A. Stern, Carlos Abellán, Waldimar Amaya, Valerio Pruneri, Thomas Jennewein, Morgan W. Mitchell, Paul G. Kwiat, Joshua C. Bienfang, Richard P. Mirin, Emanuel Knill, and Sae Woo Nam. Strong loophole-free test of local realism. *Phys. Rev. Lett.*, 115:250402, Dec 2015.

[25] Marissa Giustina, Marijn A. M. Versteegh, Sören Wengerowsky, Johannes Handsteiner, Armin Hochrainer, Kevin Phelan, Fabian Steinlechner, Johannes

Kofler, Jan-Åke Larsson, Carlos Abellán, Waldimar Amaya, Valerio Pruneri, Morgan W. Mitchell, Jörn Beyer, Thomas Gerrits, Adriana E. Lita, Lynden K. Shalm, Sae Woo Nam, Thomas Scheidl, Rupert Ursin, Bernhard Wittmann, and Anton Zeilinger. Significant-loophole-free test of bell's theorem with entangled photons. *Phys. Rev. Lett.*, 115:250401, Dec 2015.

[26] Pablo Gonzalez and Sergei Slussarenko. Challenging local realism with human choices. *Nature*, 557, 05 2018.

[27] Dominik Rauch, Johannes Handsteiner, Armin Hochrainer, Jason Gallicchio, Andrew S. Friedman, Calvin Leung, Bo Liu, Lukas Bulla, Sebastian Ecker, Fabian Steinlechner, Rupert Ursin, Beili Hu, David Leon, Chris Benn, Adriano Ghedina, Massimo Cecconi, Alan H. Guth, David I. Kaiser, Thomas Scheidl, and Anton Zeilinger. Cosmic bell test using random measurement settings from high-redshift quasars. *Phys. Rev. Lett.*, 121:080403, Aug 2018.

[28] Qiongyi He, Laura Rosales-Zárate, Gerardo Adesso, and Margaret D. Reid. Secure continuous variable teleportation and einstein-podolsky-rosen steering. *Phys. Rev. Lett.*, 115:180502, 2015.

[29] Nathan Walk, Sara Hosseini, Jiao Geng, Oliver Thearle, Jing Yan Haw, Seiji Armstrong, Syed M. Assad, Jiri Janousek, Timothy C. Ralph, Thomas Symul, Howard M. Wiseman, and Ping Koy Lam. Experimental demonstration of gaussian protocols for one-sided device-independent quantum key distribution. *Optica*, 3:634–642, 2016.

[30] Yu Xiang, Ioannis Kogias, Gerardo Adesso, and Qiongyi He. Multipartite gaussian steering: Monogamy constraints and quantum cryptography applications. *Phys. Rev. A*, 95:010101, 2017.

[31] M. D. Reid, P. D. Drummond, W. P. Bowen, E. G. Cavalcanti, P. K. Lam, H. A. Bachor, U. L. Andersen, and G. Leuchs. Colloquium. *Rev. Mod. Phys.*, 81:1727–1751, 2009.

[32] Paul Skrzypczyk, Miguel Navascués, and Daniel Cavalcanti. Quantifying einstein-podolsky-rosen steering. *Phys. Rev. Lett.*, 112:180404, 2014.

[33] Kai Sun, Xiang-Jun Ye, Jin-Shi Xu, Xiao-Ye Xu, Jian-Shun Tang, Yu-Chun Wu, Jing-Ling Chen, Chuan-Feng Li, and Guang-Can Guo. Experimental quantification of asymmetric einstein-podolsky-rosen steering. *Phys. Rev. Lett.*, 116:160404, 2016.

[34] Ioannis Kogias, Antony R. Lee, Sammy Ragy, and Gerardo Adesso. Quantification of gaussian quantum steering. *Phys. Rev. Lett.*, 114:060403, 2015.

[35] Thomas Monz, Philipp Schindler, Julio T. Barreiro, Michael Chwalla, Daniel Nigg, William A. Coish, Maximilian Harlander, Wolfgang Hänsel, Markus Hennrich, and Rainer Blatt. 14-qubit entanglement: Creation and coherence. *Phys. Rev. Lett.*, 106:130506, Mar 2011.

[36] L. K. Shalm, D. R. Hamel, Z. Yan, C. Simon, K. J. Resch, and T. Jennewein. Three-photon energy-time entanglement. *Nature Physics*, 9:19, 2013.

[37] Takao Aoki, Nobuyuki Takei, Hidehiro Yonezawa, Kentaro Wakui, Takuji Hiraoka, Akira Furusawa, and Peter van Loock. Experimental creation of a fully inseparable tripartite continuous-variable state. *Phys. Rev. Lett.*, 91:080404, 2003.

[38] Seiji Armstrong, Meng Wang, Run Yan Teh, Qihuang Gong, Qiongyi He, Jiri Janousek, Hans-Albert Bachor, Margaret D. Reid, and Ping Koy Lam. Multipartite einstein-podolsky-rosen steering and genuine tripartite entanglement with optical networks. *Nat Phys*, 11:167–172, 2015.

[39] A. T. Avelar and S. P. Walborn. Genuine tripartite continuous-variable entanglement with spatial degrees of freedom of photons. *Phys. Rev. A*, 88:032308, Sep 2013.

[40] Dik Bouwmeester, Jian-Wei Pan, Matthew Daniell, Harald Weinfurter, and Anton Zeilinger. Observation of three-photon greenberger-horne-zeilinger entanglement. *Phys. Rev. Lett.*, 82:1345–1349, Feb 1999.

[41] J. Douady and B. Boulanger. Experimental demonstration of a pure third-order optical parametric downconversion process. *Opt. Lett.*, 29(23):2794–2796, Dec 2004.

[42] Deny R. Hamel, Lynden K. Shalm, Hannes Hübel, Aaron J. Miller, Francesco Marsili, Varun B. Verma, Richard P. Mirin, Sae Woo Nam, Kevin J. Resch, and Thomas Jennewein. Direct generation of three-photon polarization entanglement. *Nature Photonics*, 8:801–807, 2014.

[43] A. S. Coelho, F. A. S. Barbosa, K. N. Cassemiro, A. S. Villar, M. Martinelli, and P. Nussenzveig. Three-color entanglement. *Science*, 326(5954):823–826, 2009.

[44] Liang Wu, Zhihui Yan, Yanhong Liu, Ruijie Deng, Xiaojun Jia, Changde Xie, and Kunchi Peng. Experimental generation of tripartite polarization entangled states of bright optical beams. *Applied Physics Letters*, 108(16):161102, 2016.

[45] Bo Jing et al. Entanglement of three quantum memories via interference of three single photons. *Nature Photonics*, 13:210–213, 2019.

[46] A. S. Bradley, M. K. Olsen, O. Pfister, and R. C. Pooser. Bright tripartite entanglement in triply concurrent parametric oscillation. *Phys. Rev. A*, 72:053805, Nov 2005.

[47] E. A. Rojas González, A. Borne, B. Boulanger, J. A. Levenson, and K. Bencheikh. Continuous-variable triple-photon states quantum entanglement. *Phys. Rev. Lett.*, 120:043601, 2018.

[48] M.K. Olsen. Third-Harmonic entanglement and Eisntein-Podolsky-Rosen steering over a frequency range of more than an octave. *Phys. Rev. A*, 97:033820, 2018.

[49] H. M. Wiseman, S. J. Jones, and A. C. Doherty. Steering, entanglement, nonlocality, and the einstein-podolsky-rosen paradox. *Phys. Rev. Lett.*, 98:140402, 2007.

[50] S. J. Jones, H. M. Wiseman, and A. C. Doherty. Entanglement, einstein-podolsky-rosen correlations, bell nonlocality, and steering. *Phys. Rev. A*, 76:052116, 2007.

[51] Lu-Ming Duan, G. Giedke, J. I. Cirac, and P. Zoller. Inseparability criterion for continuous variable systems. *Phys. Rev. Lett.*, 84:2722–2725, 2000.

[52] R. Simon. Peres-horodecki separability criterion for continuous variable systems. *Phys. Rev. Lett.*, 84:2726–2729, 2000.

[53] Vittorio Giovannetti, Stefano Mancini, David Vitali, and Paolo Tombesi. Characterizing the entanglement of bipartite quantum systems. *Phys. Rev. A*, 67:022320, 2003.

[54] M. D. Reid. Demonstration of the einstein-podolsky-rosen paradox using nondegenerate parametric amplification. *Phys. Rev. A*, 40:913–923, 1989.

[55] R. Y. Teh and M. D. Reid. Criteria for genuine N-partite continuous-variable entanglement and Einstein-Podolsky-Rosen steering. *Phys. Rev. A*, 90:062337, 2014.

[56] Peter van Loock and Akira Furusawa. Detecting genuine multipartite continuous-variable entanglement. *Physical Review A*, 67:052315, 12 2002.

[57] M. D. Reid. Monogamy inequalities for the einstein-podolsky-rosen paradox and quantum steering. *Phys. Rev. A*, 88:062108, 2013.

[58] L. Rosales-Zárate, R. Y. Teh, B. Opanchuk, and M. D. Reid. Monogamy inequalities for certifiers of continuous-variable einstein-podolsky-rosen entanglement without the assumption of gaussianity. *Phys. Rev. A*, 96:022313, Aug 2017.

[59] Christopher Gerry and Peter Knight. *Introductory Quantum Optics*. Cambridge University Press, 2004.

[60] Roy J. Glauber. Coherent and incoherent states of the radiation field. *Phys. Rev.*, 131(6):2766–2788, 1963.

[61] E. C. G. Sudarshan. Equivalence of semiclassical and quantum mechanical descriptions of statistical light beams. *Phys. Rev. Lett.*, 10(7):277–279, 1963.

[62] P. D. Drummond and C. W. Gardiner. Generalised P-representations in quantum optics. *J. Phys. A*, 13:2353–2368, 1980.

[63] Crispin W. Gardiner and P. Zoller. *Quantum Noise*. Springer, Berlin, second edition, 2000.

[64] Fritz Haake, Harald King, Guntram Schröder, Joe Haus, and Roy Glauber. Fluctuations in superfluorescence. *Phys. Rev. A*, 20(5):2047–2063, 1979.

[65] M. D. Reid and P. D. Drummond. Quantum correlations of phase in nondegenerate parametric oscillation. *Phys. Rev. Lett.*, 60:2731–2733, 1988.

[66] P. D. Drummond and P. Kinsler. Quantum tunneling and thermal activation in the parametric oscillator. *Phys. Rev. A*, 40(8):4813–4816, 1989.

[67] P. D. Drummond and A. D. Hardman. Simulation of Quantum Effects in Raman-Active Waveguides. *Europhys. Lett.*, 21:279–284, 1993.

[68] M. J. Steel, M. K. Olsen, L. I. Plimak, P. D. Drummond, S. M. Tan, M. J. Collett, D. F. Walls, and R. Graham. Dynamical quantum noise in trapped Bose-Einstein condensates. *Phys. Rev. A*, 58(6):4824–4835, 1998.

[69] C. M. Savage, P. E. Schwenn, and K. V. Kheruntsyan. First-principles quantum simulations of dissociation of molecular condensates: Atom correlations in momentum space. *Phys. Rev. A*, 74(3):033620, 2006.

[70] P. B. Blakie, A. S. Bradley, M. J. Davis, R. J. Ballagh, and C. W. Gardiner. Dynamics and statistical mechanics of ultra-cold Bose gases using c-field techniques. *Adv. Phys.*, 57:363–455, 2008.

[71] Anatoli Polkovnikov. Phase space representation of quantum dynamics. *Ann. Phys.*, 325:1790–1852, 2010.

[72] S. Kiesewetter, Q. Y. He, P. D. Drummond, and M. D. Reid. Scalable quantum simulation of pulsed entanglement and einstein-podolsky-rosen steering in optomechanics. *Phys. Rev. A*, 90:043805, 2014.

[73] Crispin W. Gardiner. *Stochastic Methods*. Springer, Berlin, first edition, 1985.

[74] Howard J. Carmichael. *Statistical methods in quantum optics 1. Master Equations and Fokker-Planck Equations*. Springer, Berlin, London, 1999.

[75] Hannes Risken. *The Fokker-Planck Equation:Methods of Solution and Applications*. Springer-Verlag, Berlin, 1996.

[76] Robert W. Boyd. *Nonlinear Optics*. Academic Press, second edition edition, 2003.

[77] P. A. Franken, A. E. Hill, C. W. Peters, and G. Weinreich. Generation of optical harmonics. *Phys. Rev. Lett.*, 7:118–119, Aug 1961.

[78] P. D. Maker, R. W. Terhune, M. Nisenoff, and C. M. Savage. Effects of dispersion and focusing on the production of optical harmonics. *Phys. Rev. Lett.*, 8:21–22, Jan 1962.

[79] J. A. Armstrong, N. Bloembergen, J. Ducuing, and P. S. Pershan. Interactions between light waves in a nonlinear dielectric. *Phys. Rev.*, 127:1918–1939, Sep 1962.

[80] Joel F. Corney, Peter D. Drummond, Joel Heersink, Vincent Josse, Gerd Leuchs, and Ulrik L. Andersen. Many-body quantum dynamics of polarization squeezing in optical fibers. *Phys. Rev. Lett.*, 97(2):023606, 2006.

[81] Peter D Drummond and Mark Hillery. *The Quantum Theory of Nonlinear Optics*. Cambridge University Press, 2014.

[82] A. Acín, D. Bruß, M. Lewenstein, and A. Sanpera. Classification of mixed three-qubit states. *Phys. Rev. Lett.*, 87:040401, Jul 2001.

[83] Jean-Daniel Bancal, Nicolas Gisin, Yeong-Cherng Liang, and Stefano Pironio. Device-independent witnesses of genuine multipartite entanglement. *Phys. Rev. Lett.*, 106:250404, Jun 2011.

[84] A. S. Villar, M. Martinelli, C. Fabre, and P. Nussenzveig. Direct production of tripartite pump-signal-idler entanglement in the above-threshold optical parametric oscillator. *Phys. Rev. Lett.*, 97:140504, 2006.